



# Mineral Mapping

## **Interpretation of Multielement Geochemistry and SWIR mineralogy from the Que River – Hellyer area.**

**Scott Halley**

21/11/2009

## Summary

Identifying losses and gains of chemical components due to hydrothermal alteration depends on firstly recognizing what the starting composition of the rock was. The immobile trace elements were used to classify the primary compositional varieties within the Que-Hellyer Volcanics. Within each compositional group, gross changes in chemical composition were tracked using molar ratio plots of K/Al vs Na/Al. From this, the relative changes in proportions of albite, sericite and K-feldspar were tracked graphically.

Proximal alteration at Hellyer, Que River and Mt Charter is characterized by very strong sodium depletion. The most strongly altered rock is intensely sericitised, but may also contain Mg-chlorite or K feldspar. The sodium depletion is an acid alteration signature, but the K feldspar and Mg chlorite is an alkaline overprint. The alkaline overprint may be due to down draw and fluid mixing with cold seawater within the alteration pipes. Que River has a wide and intense footwall alteration system, with quite sharp boundaries. The Hellyer footwall alteration is much narrower, but the surrounding halo is significantly sodium enriched. Mt Charter has a very strong albite halo.

As well as the sodium depletion, Ca and Sr are also strongly depleted in proximal areas. Ba is depleted in strongly sericitised rocks, but enriched in the albitic halo zone, so it forms a donut pattern around the footwall alteration. Mg and Li are depleted in the sericite zones, but become enriched in the proximal footwall Mg-chlorite zones. Mn is depleted in the sericite zones, but the ferroan carbonates associated with the proximal footwall alteration are also Mn-bearing.

The sulfide mineralogy has a very significant control on the distribution patterns of the chalcophile pathfinder elements. Base metal sulfides have an irregular distribution, so Cu, Pb and Zn do not form regular patterns. The pathfinder elements that are hosted by pyrite, on the other hand, form exceptionally coherent patterns. Think of this in terms of sampling statistics; 30cm sample of core may or may not have a few grains of chalcopyrite or sphalerite, and this will be the difference between background Cu or Zn values, or several hundred ppm. However, the same piece of core may have a hundred or more pyrite, so the elements hosted in the pyrite always give a positive result. The proximal pyrite has a very distinctive As-Sb-Tl signature. Ag, Bi, W and Sn also give quite coherent patterns, although not as consistent as As-Sb-Tl. It is likely that a significant amount of the low level anomalous Ag is also hosted in pyrite. Bi, Te and Sn are more anomalous in deeper parts of the stringer zones, whereas As, Sb and Tl are most abundant in the shallow levels of the stringer zones, underneath the massive sulfide lenses.

The litho-geochemistry results provide a great insight to the historic soil geochemistry results. The arsenic trends in the soil geochemistry are a very good match for the arsenic from the litho-geochemistry, but the soil geochemistry provides a full field coverage. Copper and zinc in particular map the lithology (highly correlated with Fe) and don't give a positive response or anomalous footprint until the samples are right on top of the massive sulfide lenses. There are some coherent Pb-Zn anomalies that don't have a supporting As response, but these might be due to a different metallogenic event.

The spectral results were more complex than anticipated. Rather than the stringer zones being characterized by short wavelength, acid type micas, they turned out to have some exceptionally long wavelength micas. The shallow parts of the stringer zones in proximity to the sulfide lenses at Hellyer Fossey and Mt Charter are characterized by exceptionally long wavelength sericite, particularly around the K feldspar bearing zones. However, the albitised haloes are also phengitic. Deeper levels of the stringer zones generally have shorter wavelength sericite. Sericite formed under "rock-buffered" conditions has mid-range wavelengths. The entire rock package bounded to the south by the Mt Cripps fault, the Henty Fault and bounded to the west by the Que-Hellyer corridor stands out as a domain of short wavelength, muscovitic micas. This is also a domain of long wavelength Fe-rich chlorites. The mineralized corridor is a domain of short wavelength, Mg-rich chlorite. However, this is not a unique signature either, as the albitised halo also contains short wavelength, Mg-rich chlorite.

The most diagnostic signatures are elevated As-Sb-Tl, sodium depleted sericite +/- chlorite, KSpAr mineralogy, and elevated sulfur (pyrite).

On the basis of these criteria, the selected targets are;

- northern extension of Hellyer
- D-Zone
- Que South
- HL629
- Switchback area
- Amoeba zone
- Barite Creek.

Summary.....	2
Bass Metals Lithogeochemistry .....	6
Primary rock-type Classification.....	6
Alteration Classification.....	11
Pathfinder Elements.....	14
Correlations between Spectral Data and Geochemical Data.....	19
Soil Geochemistry.....	25
Signatures of Hellyer and Que River.....	28
Targets.....	34
References .....	44
Figure 1. Correlations between Fe and Sc and V. ....	6
Figure 2. Immobile trace element plots used to classify the primary rock types. ....	7
Figure 3. Immobile trace element plots with point density contour overlays.....	8
Figure 4. Immobile trace element trends. ....	9
Figure 5. Classification of immobile trace element groups. ....	10
Figure 6. Alteration plot for andesites.....	11
Figure 7. map of alteration mineralogy derived from a "General Element Ratio" plot. ....	12
Figure 8. Sodium plot from Hellyer showing the sodium depletion around the ore zone, and spotty sodium enrichment plotting as a halo.....	13
Figure 9. Reaction path of acid alteration, with loss of Na followed by loss of Ca. ....	13
Figure 10. Comparison of antimony distribution vs zinc distribution. ....	14
Figure 11. Antimony and Thallium maps for the area from Hellyer to Mt Charter. ....	15
Figure 12. Probability plots of As, Sb, S and Tl, coloured by alteration type.....	16
Figure 13. Thallium versus Potassium .....	17
Figure 14. Log-Log correlation between Tl and Sb.....	18
Figure 15.....	19
Figure 16.....	20
Figure 17.....	20
Figure 18.....	21
Figure 19.....	22
Figure 20.....	23
Figure 21.....	24
Figure 22.....	25
Figure 23.....	25
Figure 24.....	26
Figure 25. Map of Arsenic in soils.....	27
Figure 26. Map of Copper in soils.....	27

Figure 27. Que River Alteration Mineralogy .....	28
Figure 28. Que River ASD Mineralogy .....	28
Figure 29. Que River Sulfur geochemistry. ....	29
Figure 30. Que River Thallium geochemistry. ....	29
Figure 31. Que River sericite wavelengths. Blue<2200nm, Red>2215nm.....	30
Figure 32. Que River chlorite wavelengths. Blue<2251nm, Red>2257nm .....	30
Figure 33. Hellyer Alteration Mineralogy .....	31
Figure 34. Hellyer ASD Mineralogy.....	31
Figure 35. Hellyer Sulfur geochemistry. ....	32
Figure 36. Hellyer Thallium geochemistry .....	32
Figure 37. Hellyer sericite wavelengths. Blue<2200nm, Red>2215nm.....	33
Figure 38. Hellyer chlorite wavelengths. Blue<2251nm, Red>2257nm .....	33
Figure 39. Target zones north of Hellyer; plan view. ....	34
Figure 40. Target zones north of Hellyer; Thallium geochemistry; plan view. ....	35
Figure 41. Target zones north of Hellyer; Arsenic geochemistry; plan view. ....	35
Figure 42. Alteration mineralogy north of Hellyer; section view.....	36
Figure 43. D Zone alteration mineralogy projected to plan view. ....	36
Figure 44. D Zone alteration mineralogy projected to section view. The shapes are the upper basalt from the Geoinformatics model.....	37
Figure 45. Alteration Mineralogy projected to plan view; Que South. ....	37
Figure 46. Antimony geochemistry projected to plan view; Que South. ....	38
Figure 47. Que South Thallium geochemistry projected to a section. the shape is the upper basalt from the Geoinformatics 3D model.....	38
Figure 48. HL629 alteration geochemistry projected to plan view.....	39
Figure 49. HL629 Thallium geochemistry projected to plan view.....	39
Figure 50. HL629 alteration mineralogy projected to cross section. The shape is the upper basalt from the Geoinformatics 3D model.....	40
Figure 51. Arsenic soil geochemistry across the Switchback Zone. ....	40
Figure 52. Arsenic geochemistry in HED12, Switchback area .....	41
Figure 53. Arsenic soil geochemistry; Amoeba Zone. ....	42
Figure 54. Arsenic soil geochemistry; Barite Creek.....	43

## Bass Metals Lithochemistry

3500 samples were collected from 186 exploration drill holes. All the exploration drill holes outside of the Que River and Hellyer resource areas were sampled at intervals of around 15m. Obvious veins were avoided. The objective was to characterize the primary host rock and the alteration superimposed upon it. The samples were analysed by Amdel using a 4 acid digest, and a combined ICP/MS-AES assay method. A comparison between the assay results and analyses from Crawford et al (1992) which defined the Suite1 to Suite5 scheme shows that the 4 acid digest is close to a complete digest for most elements, including Ti and Zr. The Cr assays could be 20% below total Cr.

## Primary rock-type Classification

The immobile trace elements were used to classify the samples into geochemical populations. To do this, numerous scatterplots of the immobile trace elements were generated to look for populations or groupings within the data. Sc and V are particularly useful. They substitute for Fe into pyroxenes and amphibole, but they are much less mobile than Fe during alteration and weathering (figure 1). Sc and V can therefore be used as proxies for the primary Fe content of the rock. V can also substitute into Fe oxides, (eg, into magnetite), so magnetite fractionation will change the Fe:V correlation.

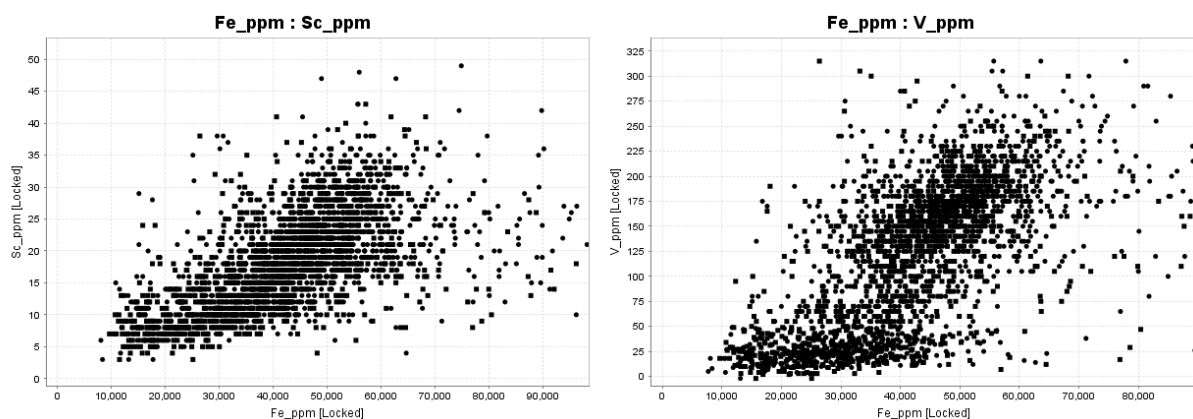
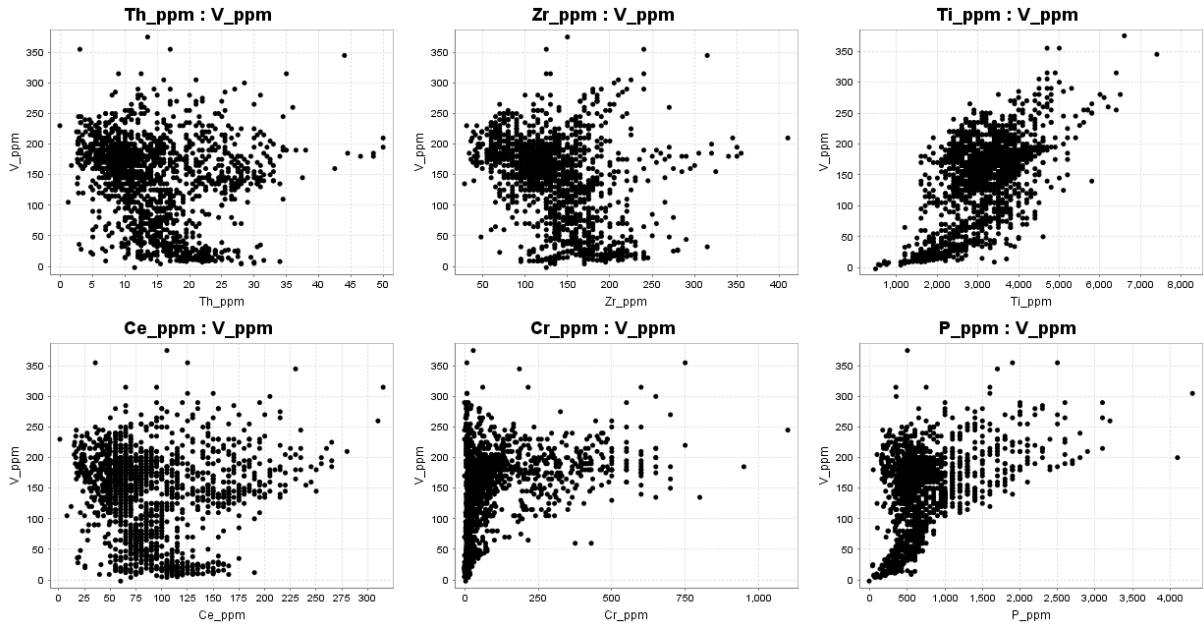


Figure 1. Correlations between Fe and Sc and V.

On the basis of the V, Ti, Zr, Cr, P and Th contents, the rocks were classified into;

- rhyolites,
- dacites,
- andesites,
- low Zr-high Cr basalts,
- LREE-enriched basalt suite (which has very variable Cr contents).



**Figure 2. Immobile trace element plots used to classify the primary rock types.**

One of the very distinctive features of the Que-Hellyer volcanics is the presence of exceptionally P-La-Ce-Th rich intermediate to mafic rocks. These are the Suite2 and Suite3 series identified by Crawford et al (1992). The suite3 rocks have around 150ppm Ce compared to 50ppm in the suite1 andesites, and 20ppm Th compared to 10ppm in the andesites.

Another very distinctive feature is the range of Cr values, especially some of the high Cr contents in the basalts. There is a broad range of Cr contents, although these plot in clustered groups that probably define individual flow units. The combination of high Cr, and very strong LREE enrichment indicates that the Suite2 and Suite3 magmas were derived from an enriched mantle source.

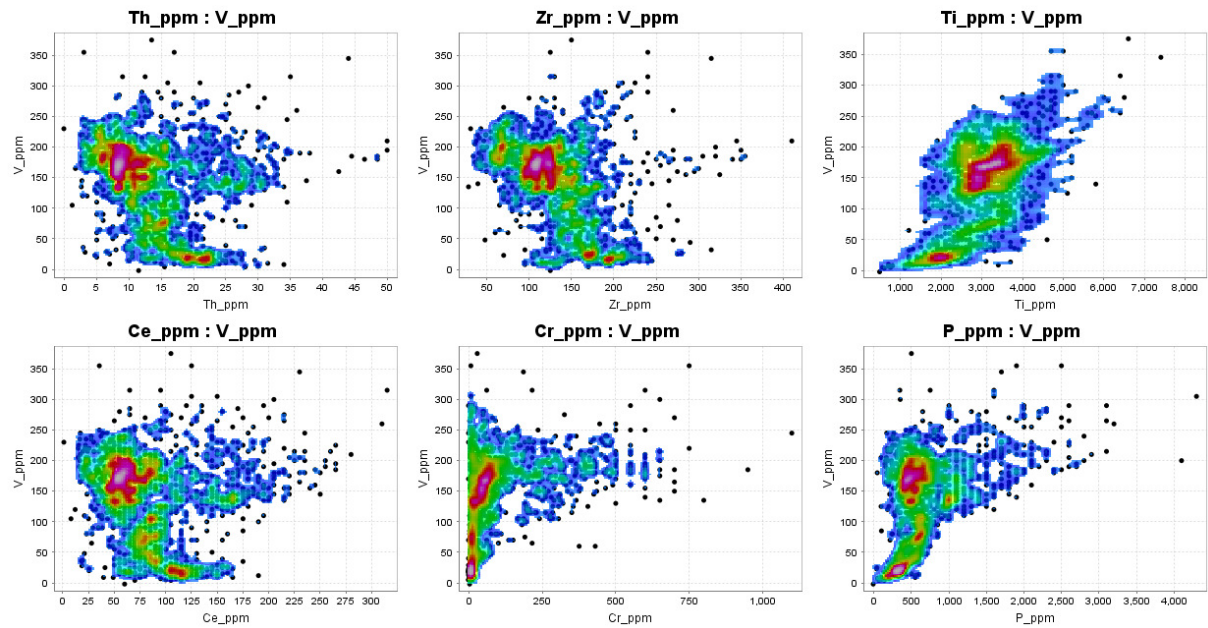


**Figure 3. Immobile trace element plots with point density contour overlays.**

From the logging codes, the clastic (fragmental) and stringer zone rocks were deselected, so that in the first pass, only coherent facies, weakly to moderately altered rocks were considered. The immobile trace element signatures of these rocks are plotted in figure 2. The same plot is shown in figure 3 with a point density overlay to highlight the clusters in the data. The clusters highlighted in figure 3 were colour-coded, and then cross checked from plot to plot to check for consistency (figures 4, 5).

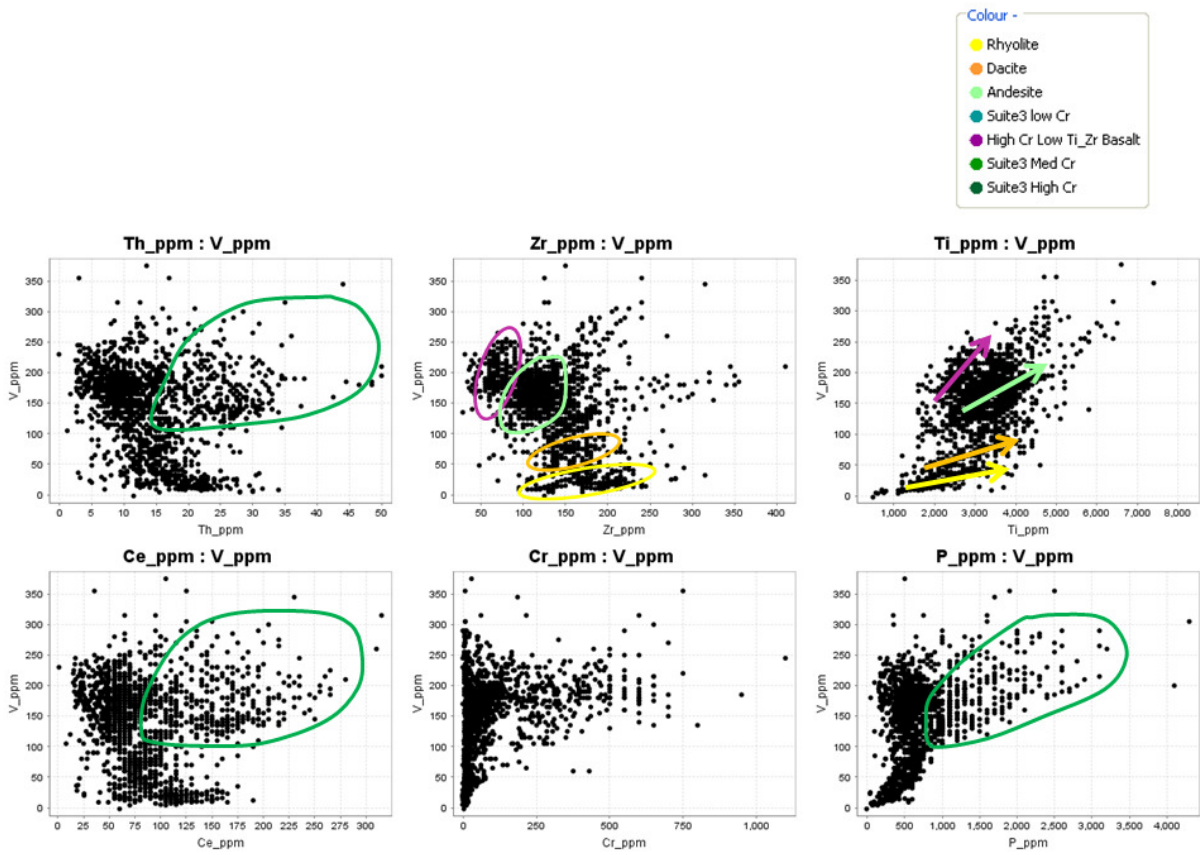


Figure 4. Immobile trace element trends.

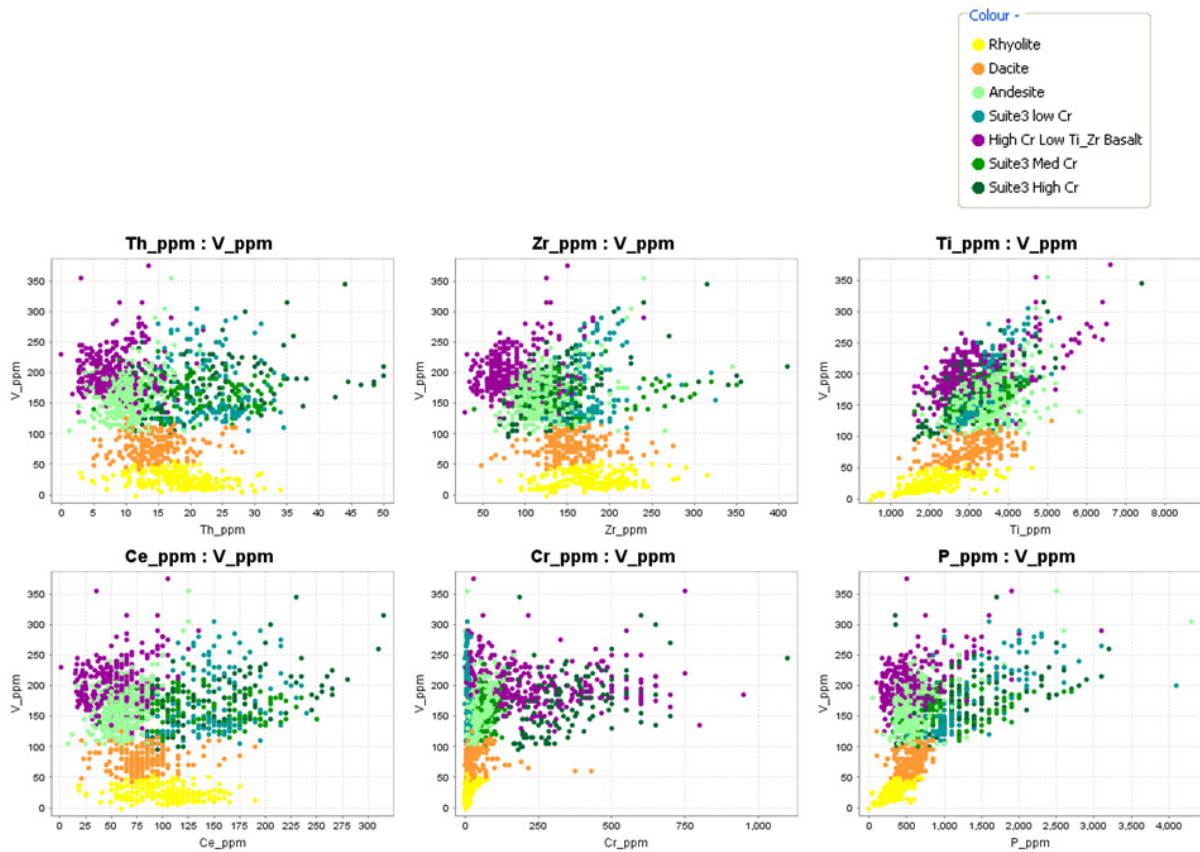


Figure 5. Classification of immobile trace element groups.

Figure 5 shows the classification of the groups that was made on the basis of these plots. There is some overlap between the groups, so the classification is not 100% accurate. Somewhere around 10% of the points are ambiguous within this scheme. Following this classification, the more altered samples and fragmental rocks were overlaid, and assigned to groups within the same scheme.

The suite3 rocks were subdivided on the basis of their Cr content. At a local scale, this will probably map individual flow units. An alternative would have been to subdivide them on the basis of the LREE and/or Th and/or P content.

## Alteration Classification

A convenient way to quantify the chemical changes during alteration is to plot the whole rock analyses as general element ratios of K/Al vs Na/Al (figure 6). These are ratios calculated on a molar proportion rather than a weight percent basis. This allows the data to be projected in terms of alteration mineral compositions. In this way, the relative amount of sericite, or albite can be quantified. Each rock type has a different primary composition, so a separate projection is required for each compositional group. Once the alkali-element alteration trends have been identified within each compositional group, all of the data can be re-combined to see the overall alteration picture.

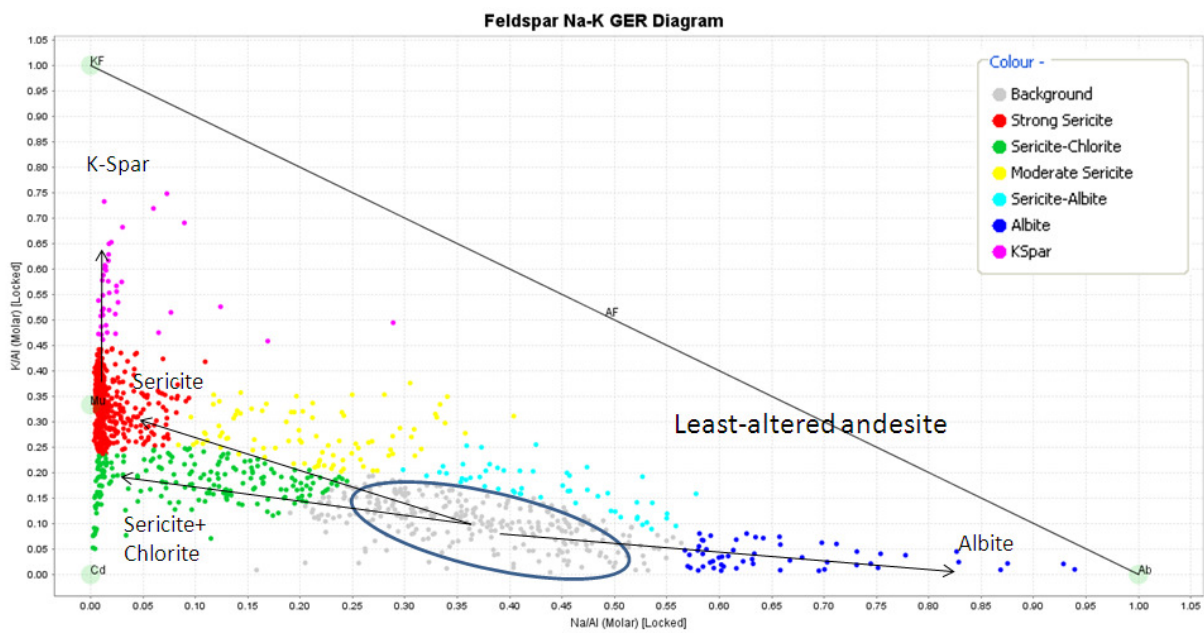


Figure 6. Alteration plot for andesites.



Figure 7. map of alteration mineralogy derived from a "General Element Ratio" plot.

Figure 7 shows the geochemical alteration signatures in plan view. The "Strong Sericite" and "Sericite-Chlorite" groups are very strongly sodium depleted. These define a corridor from north of Hellyer to south of Que River, and then another cell at Mount Charter. Que River has a halo of moderate sericite-chlorite. Hellyer has a strong sericite core, but then a halo of sodium enrichment (albite). In the halo around Hellyer, the sodium contents average around 5% Na<sub>2</sub>O compared to a background of around 3.5% Na<sub>2</sub>O. In places, the boundary between sodium depletion and sodium enrichment is very sharp. The albite halo around Mt Charter is even more pronounced. The albitised zones report in the spectral data as phengite. One interpretation of the localized albite haloes is that they are the result of shallow level "piggy-back" convection cells of sea water.

Phengitic micas can have a maximum K:Al ratio, on a molar basis, of 0.45. Quite a few of the data points are strongly sodium depleted, but have a K:Al ratio greater than 0.45. These samples must contain an extra K-bearing mineral. This will be K-Spar. This occurs in very proximal positions at Fossey, Mt Charter, D-zone and Que South.

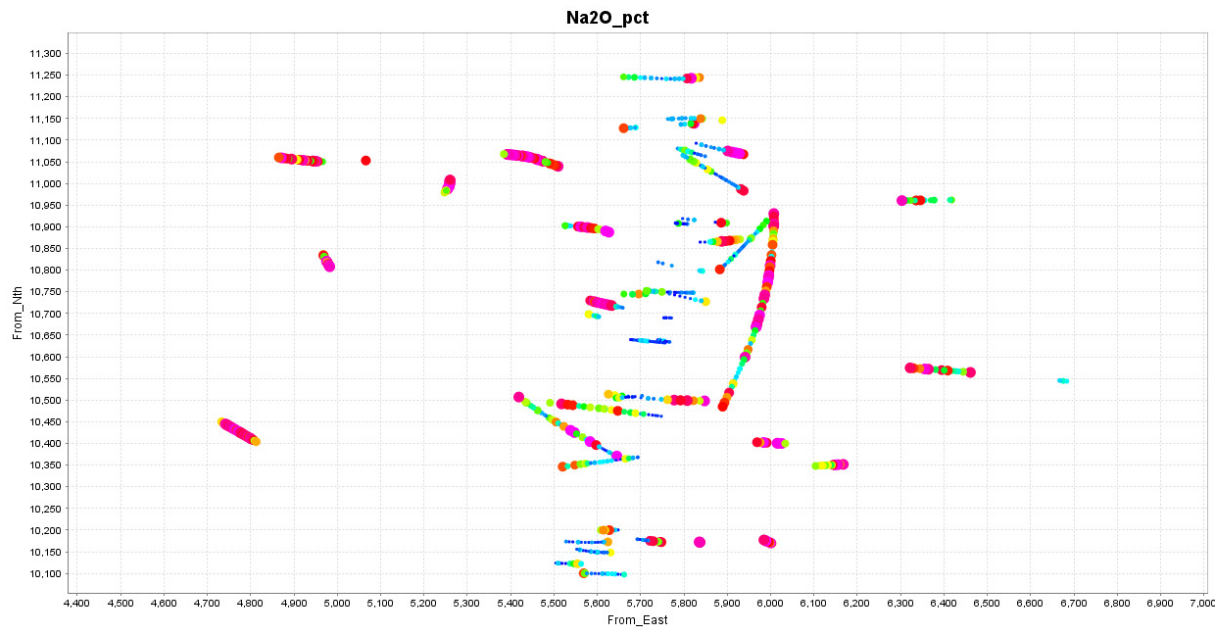


Figure 8. Sodium plot from Hellyer showing the sodium depletion around the ore zone, and spotty sodium enrichment plotting as a halo.

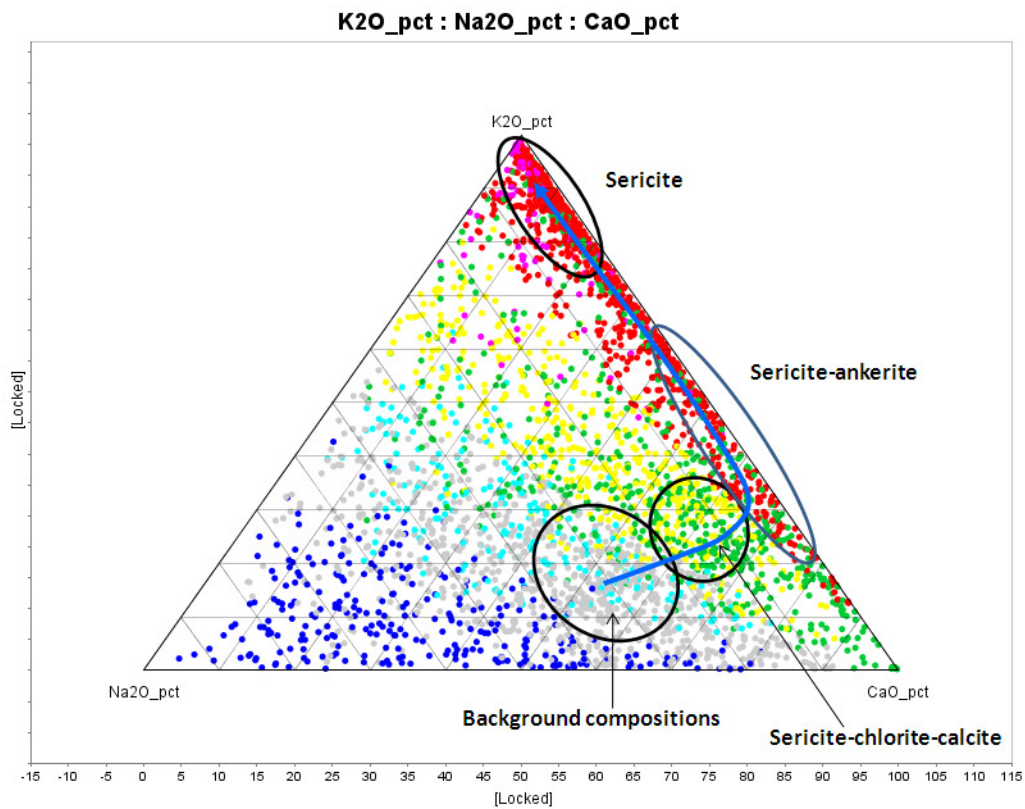


Figure 9. Reaction path of acid alteration, with loss of Na followed by loss of Ca.

A ternary plot of K-Na-Ca shows that the moderately sericite-chlorite altered rocks retain Ca (as calcite), and some of the strongly sodium depleted rocks still have significant Ca contents. In the drill core, pervasively sericitised core commonly contains ankerite. However, in the most intensely sericitised rocks, Ca is also totally depleted, so eventually, the ankerite is lost as well.

## Pathfinder Elements

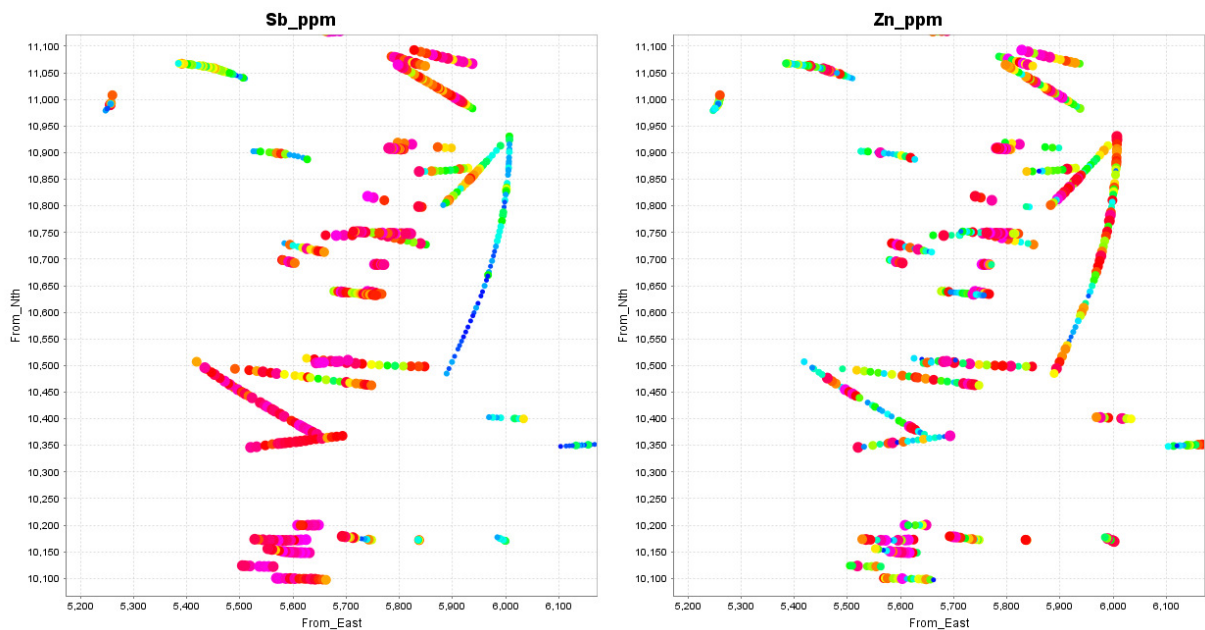


Figure 10. Comparison of antimony distribution vs zinc distribution.

Figure 10 is a very informative plot. Consider the mineralogy that controls the distribution of these elements. Zinc has a background of 50 to 100ppm in basalts. Levels above this will be controlled by sphalerite. A few grains of sphalerite in a sample will give an assay result of maybe 500ppm (which is at the high end of the results in this data). However, the sphalerite is irregularly distributed, so there are “false negatives” within the Hellyer system, and “false positives” outside the footprint of Hellyer.

Irregularly distributed minerals like sphalerite, galena and chalcopyrite don't give rise to very coherent geochemical patterns. The most coherent patterns come from elements which substitute into very widely distributed alteration minerals. Pyrite acts as a host to lots of different metals including As, Sb, Mo, Bi, Te, Tl to name a few. A 30cm stick of drill core might contain just a few grains of galena or sphalerite, but may contain hundreds of pyrite grains. Therefore, for those elements hosted by pyrite, the variance in the assay values will be very low. That is, the chemical patterns should be very coherent, and very “contourable”. Figure 10 shows that antimony maps the distribution of ore-related pyrite and gives a remarkably coherent pattern, but sphalerite has an erratic distribution outside of the ore bodies and as such, is a poor pathfinder element.

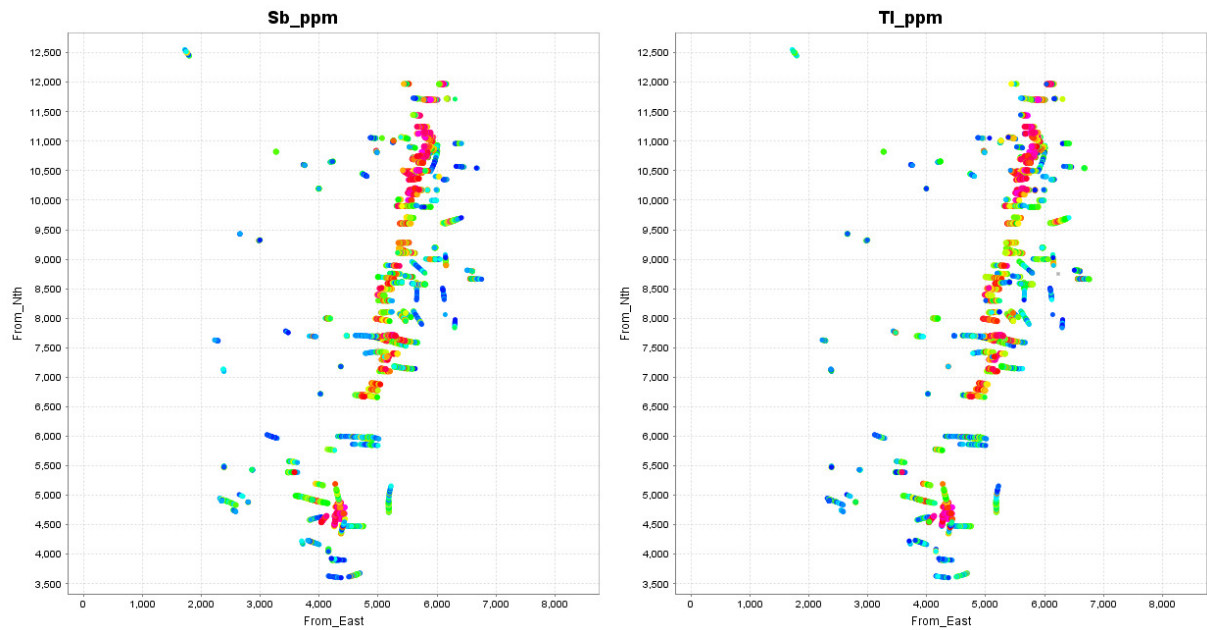


Figure 11. Antimony and Thallium maps for the area from Hellyer to Mt Charter.

The elements that work particularly well in the Hellyer-Que River area are arsenic, antimony and thallium (figure 11). These elements clearly define the proximal footprint of Hellyer, Que River and Mt Charter. They also define a corridor from north of Hellyer to south of Que River. These elements clearly define the distribution of the VMS-related pyritic halo.

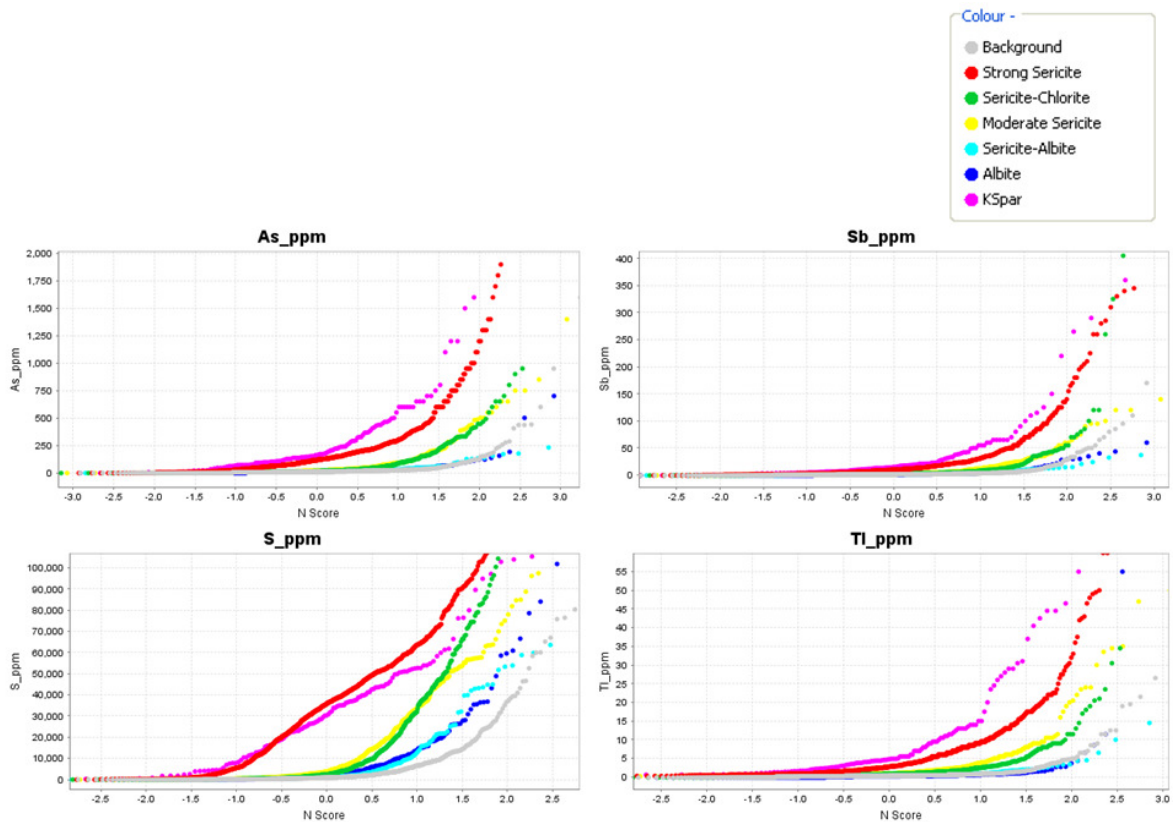


Figure 12. Probability plots of As, Sb, S and Tl, coloured by alteration type.

Probability plots (figure 12) are a very useful way to look at the correlation between alteration (silicate mineralogy) and pathfinder chemistry. In a probability plot, the N-score is plotted against the assay value. N-score is the  $(\text{assay} - \text{median}) / \text{standard deviation}$ .

At a given N-score value, observe which alteration types carry the highest values of As, Sb, S and Tl. The K-Spar zones have the highest As-Sb-Tl, but there is slightly more pyrite on average, in the strong sericite zones. Note also that the albite-bearing rocks can be quite pyritic in places, but the pyrite in the albite zones carries less As-Sb-Tl. The probability plots show that not all of the pyrite is the same. Measuring As-Sb-Tl is not just a reflection of the total pyrite content.

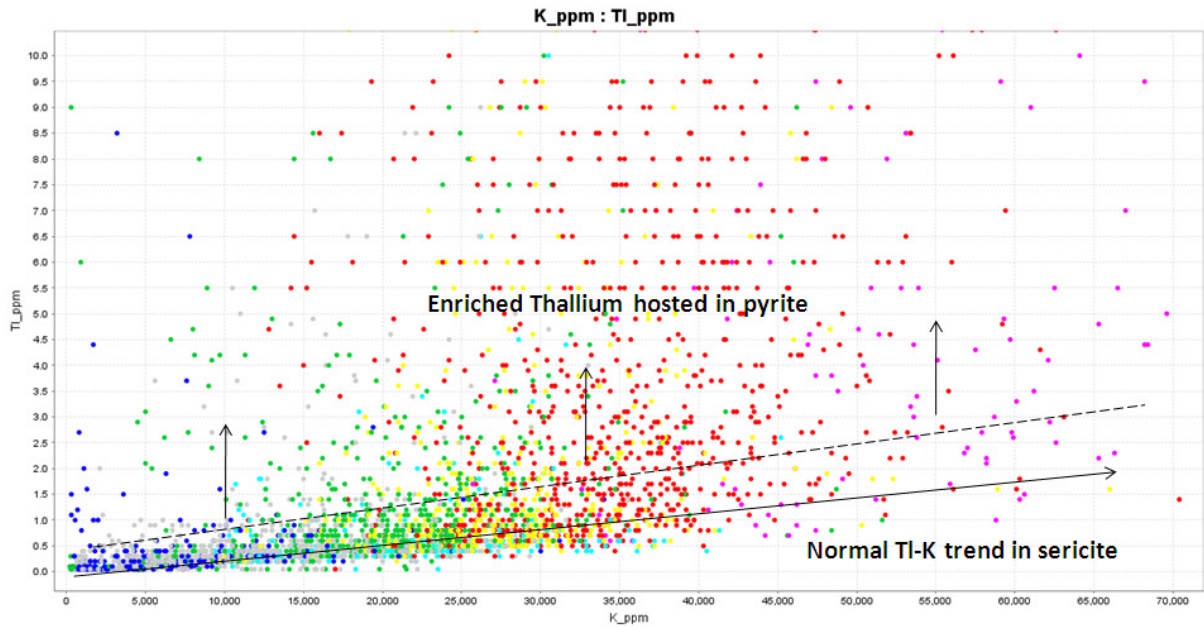


Figure 13. Thallium versus Potassium

The thallium content in the Hellyer camp is particularly interesting. In 99% of data sets, Tl is highly correlated with K. This is because the usual host for thallium is sericite, where Tl substitutes for K. However, thallium has a very unusual property in that it can also substitute into pyrite. Figure 13 shows a cloud of points with a strong linear trend. Along this trend, at 4% K there is 1ppm Tl. This is the sericite hosted thallium. The points plotting above this trend have thallium hosted in pyrite. The Carlin deposits are another example of mineral systems with Tl-rich pyrite. Figure 14 shows that thallium and antimony are highly correlated and both metals have the same behaviour with respect to their substitution into pyrite.

Ag, Bi, W, Sn and Te all work to some extent as proximal pathfinders, but none of these work anywhere near as well as As-Sb-Tl. Besides Na and Ca, there are demonstrable depletions in Mn, Co, Ni and Ba in the proximal footwall alteration.

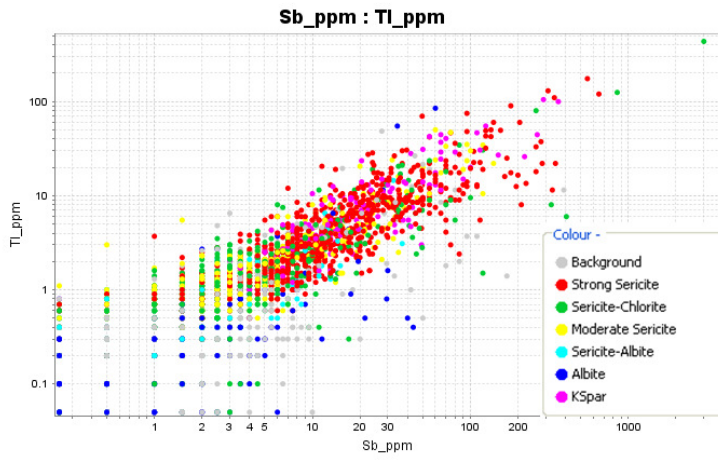


Figure 14. Log-Log correlation between Tl and Sb

## Correlations between Spectral Data and Geochemical Data

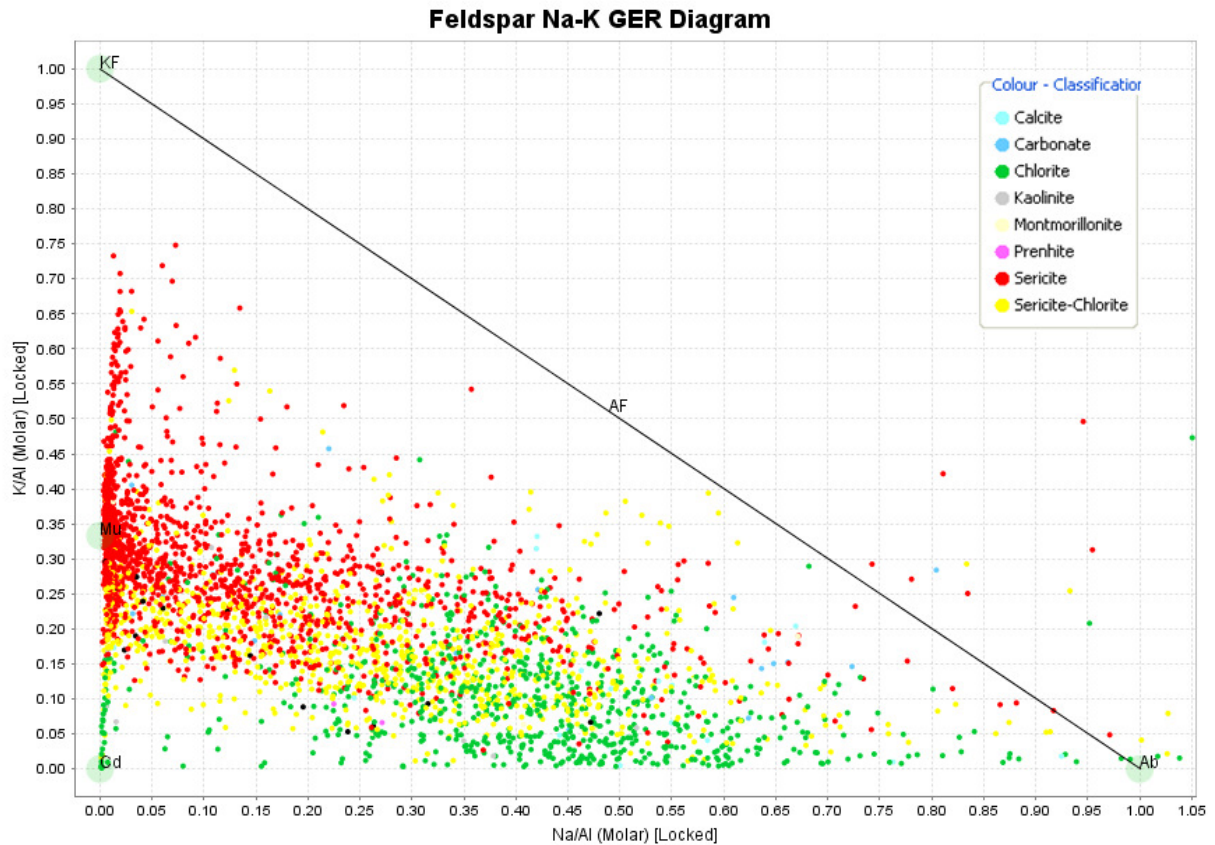


Figure 15.

Figure 15 shows the Albite-Sericite general element ratio plot. This plot is based on the lithochem assay results, but the points are coloured by the mineralogy classes determined from the ASD. Note that the sample points that are closer to the albite-rich end of the data spread are dominantly chloritic; ie chlorite-albite. Imagine a tie-line that joins the projected positions of albite and muscovite. The points closest to this tie line are mostly plotting as sericite (red points), but further below the tie line, yellow, and then green points (chlorite) become more common. Notice also that there are two domains of chlorite; one domain where chlorite occurs in albite-bearing rocks, and another domain where chlorite occurs in very strongly Na-depleted rocks.

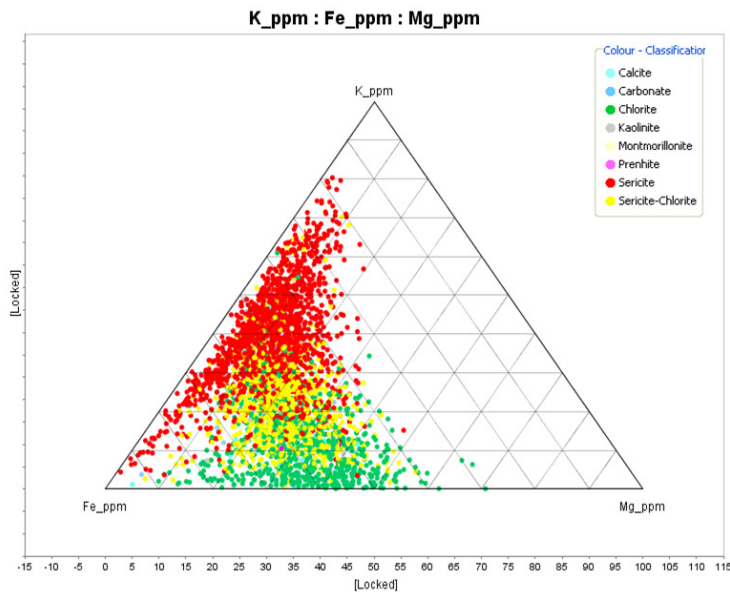


Figure 16.

Figure 16 shows that the progressive reaction from albite plus chlorite (green) to sericite plus chlorite (yellow) to sericite (red), is accompanied by magnesium depletion, although for the vast majority of samples, the Fe content remains more or less the same. The exception is the domain where chlorite occurs in the strongly Na-depleted rocks. These rocks are Mg-enriched. This is best illustrated in figure 17. This is a K-Mg-Na ternary plot. Just the andesitic rocks are shown here so that the trends are not masked by variable host rock compositions.

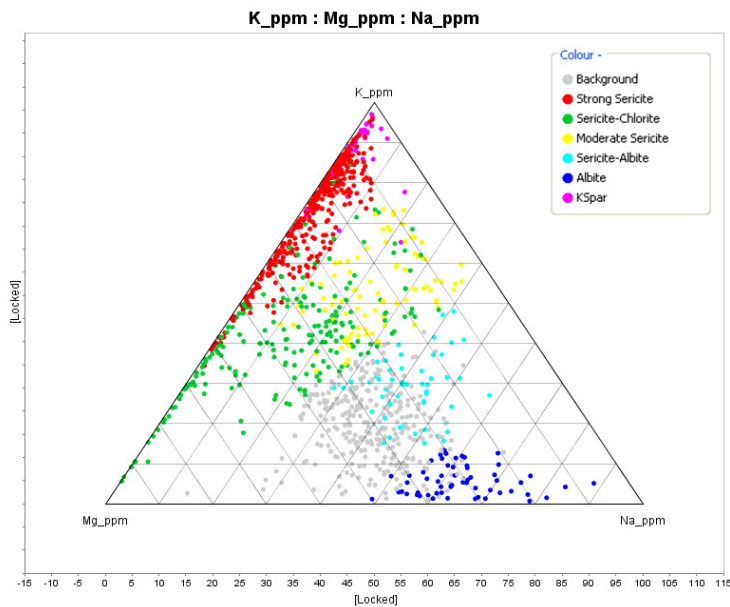


Figure 17.

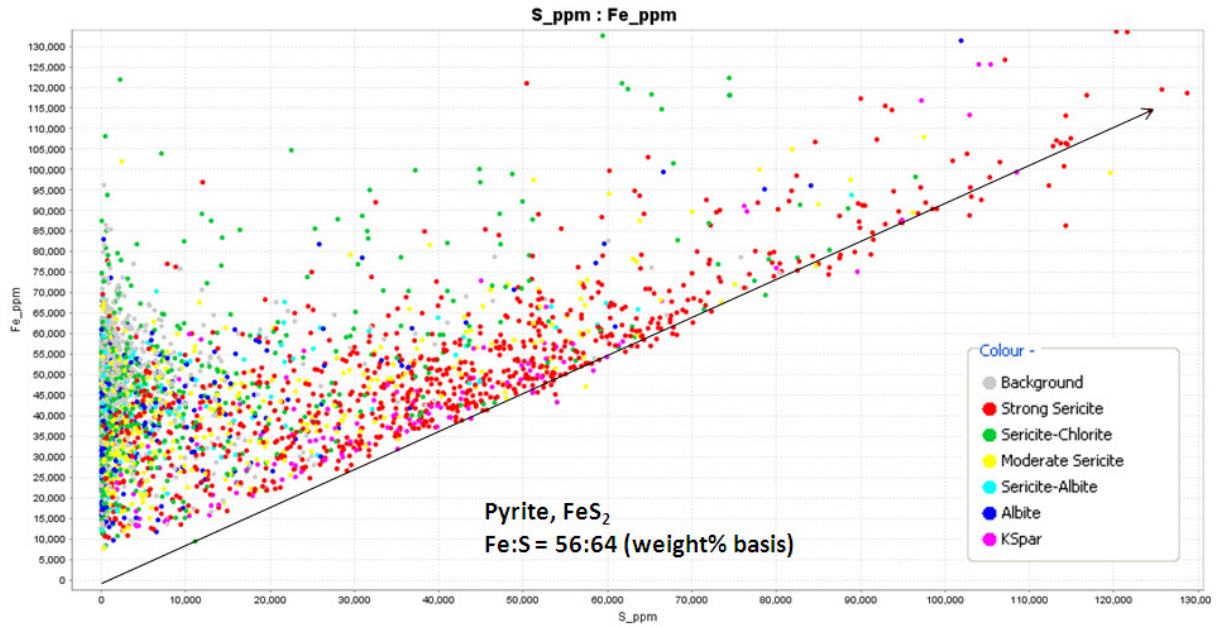


Figure 18.

Figure 18 shows that the formation of pyrite generally only uses the Fe that is already in the rock. Within a given compositional group, eg basalt or andesite, the Fe content of a completely sulfidised rock is more or less the same as its unaltered equivalent. There are a small percentage of samples that show a pronounced Fe enrichment.

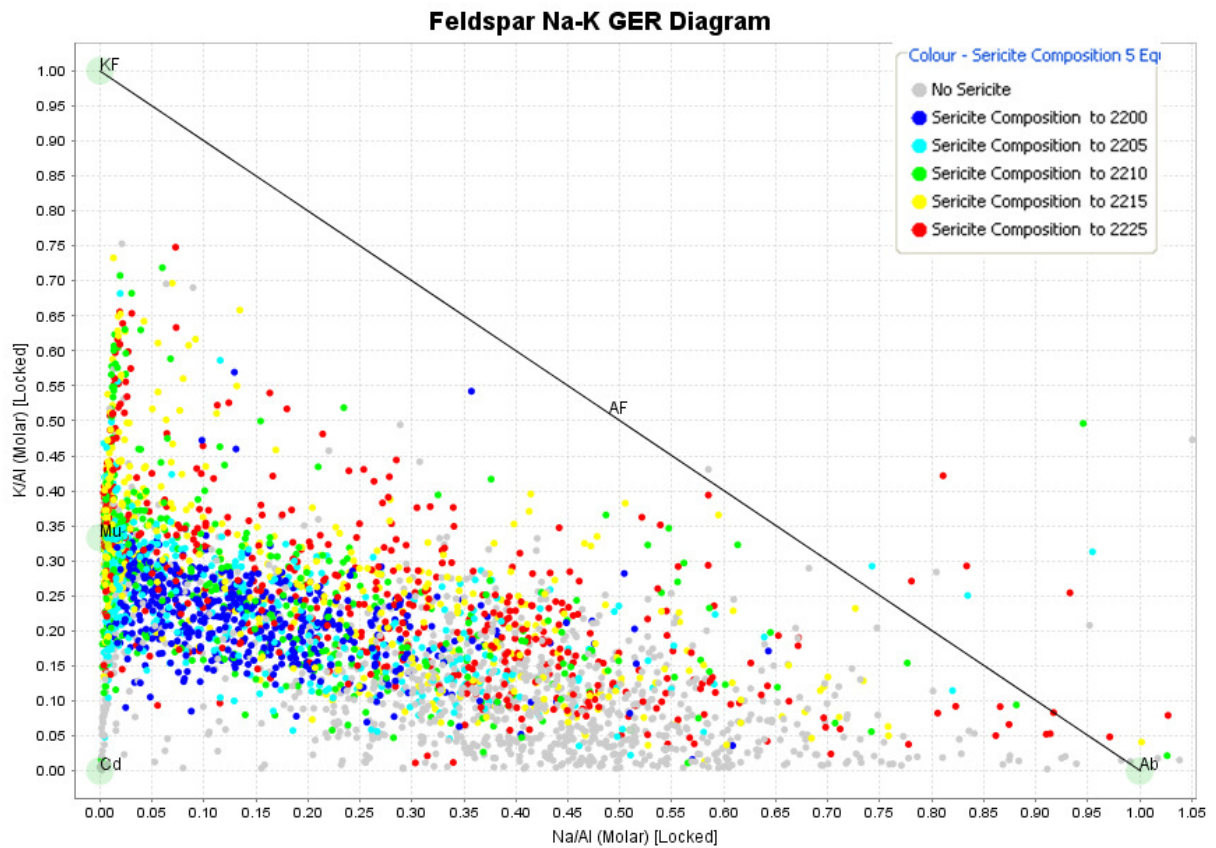


Figure 19.

Figure 19 shows the Albite-Sericite general element ratio plot again. The plot is based on the lithogeochem assay results, but this time the points are coloured by the wavelength of the 2200nm absorption feature in the sericite-bearing samples. Note that the short wavelength samples occur in the points that plot below the muscovite-albite tie line. The longer wavelength micas occur either at the more sodic end of the composition ranges, or above the albite-muscovite tie lie, heading into a K feldspar domain. Hence, there are 2 different chemical domains for phengite (long wavelength mica); a sodic domain and a potassic domain.

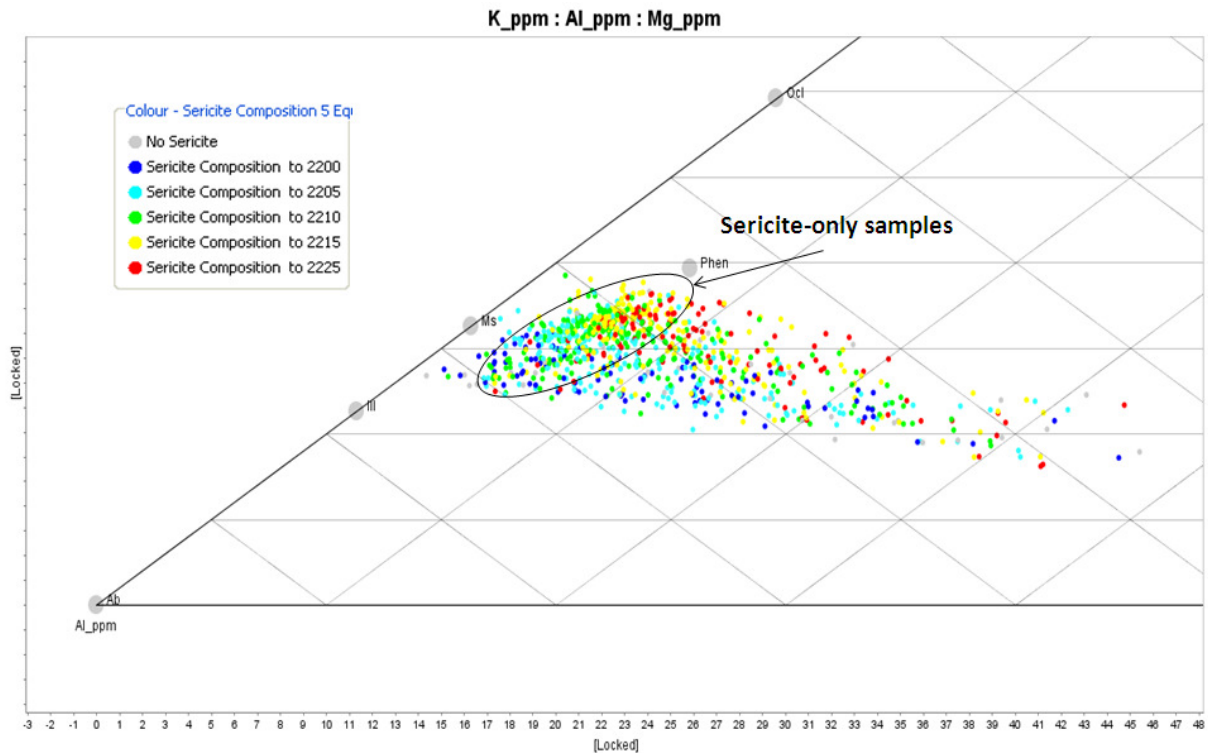
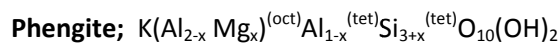
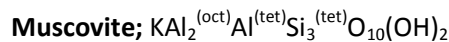


Figure 20.

Consider some theoretical end members for sericite types; muscovite, phengite and illite. In figure 20, all the points that plot in the “strong sericite group” from figure 6 have been plotted on a ternary diagram of K-Al-Mg, and the points are coloured by the wavelength of the 2200nm feature. The projected positions of the sericite end-member compositions are also shown on this plot.



In figure 20, there is a cluster of points mapping a trend between phengite and illite. These are the samples that contain only sericite. The trail of points heading to more Mg-rich compositions contains traces of chlorite as well as sericite. Within the sericite-only samples, the phengite-rich end has long wavelength 2200nm features, and the illite-rich end has short wavelength 2200nm wavelengths. It is interesting that the short wavelength end is trending towards slightly illitic rather than just stoichiometric muscovite. This plot provides confirmation that the wavelength shift in the micas really is mapping the phengite to muscovite solid solution.

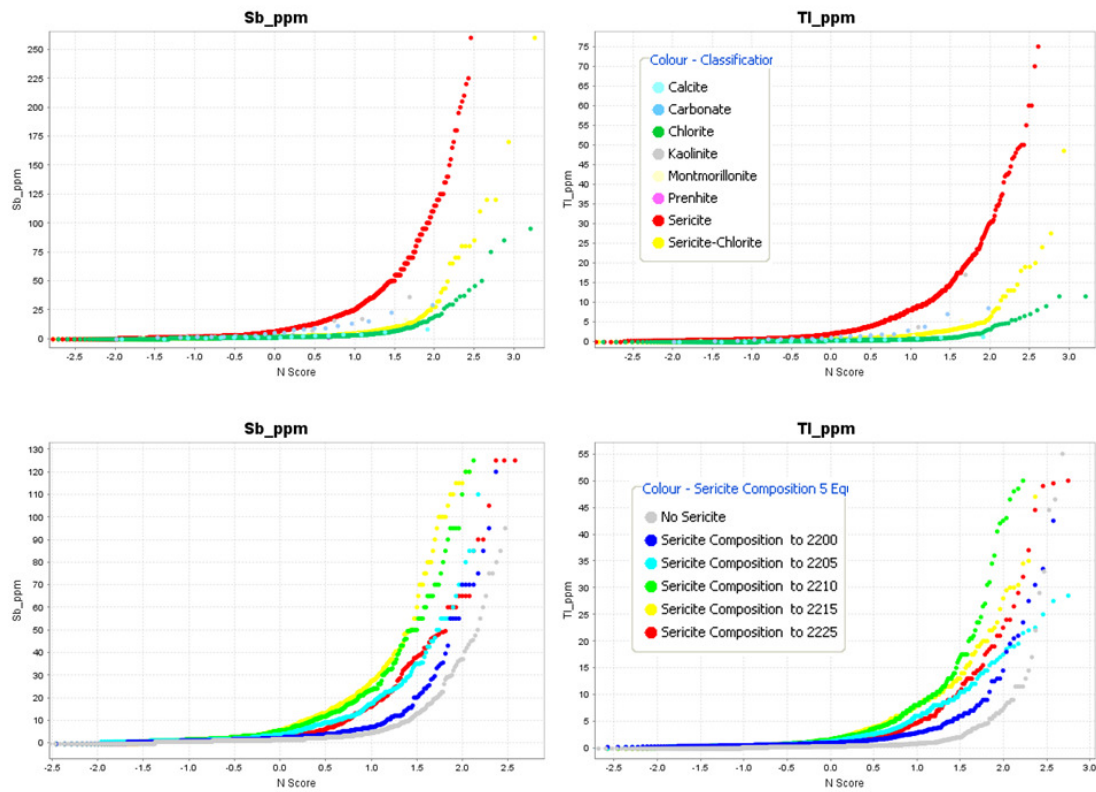


Figure 21.

Figure 21a shows probability plots for Sb and Tl coloured by the ASD mineralogy. This shows that these elements are very strongly biased towards sericite-rich alteration. In figure 21b, the Sb and Tl probability plots are coloured by the wavelengths of the 2200nm feature in the sericite. Perhaps surprisingly the strongest pathfinder signals occur with mid-range wavelengths rather than long or short wavelengths. One interpretation of this would be that the metals are transported in acid fluids, but precipitation of pyrite and associated pathfinders in the near-ore environment is strongly influenced by neutralization of the acidity as well as temperature decrease.

## Soil Geochemistry

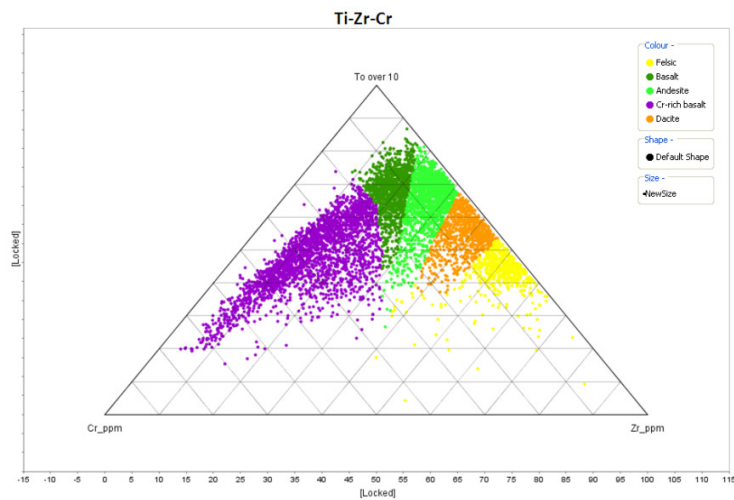


Figure 22.

Quite a few of the soil samples collected by Aberfoyle were assayed for Ti, Cr and Zr as well as a suite of base metals. The immobile elements show a spectrum of compositions from rhyolite to Cr-rich basalt. The points have been classified into felsic, dacite, andesite, basalt and Cr-rich basalt, based on the identification of point density clusters with figure 22. Even though this is a simplistic classification, and the signatures are “smeared” in the soils, this provides a reasonable match with the interpreted geology (figure 23).

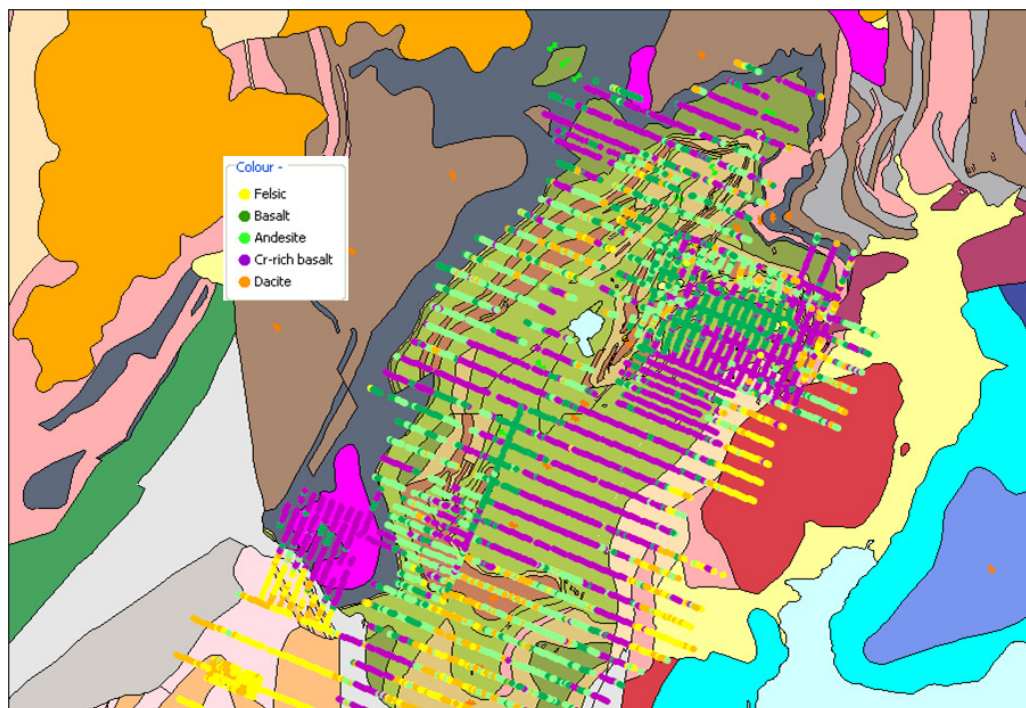


Figure 23.

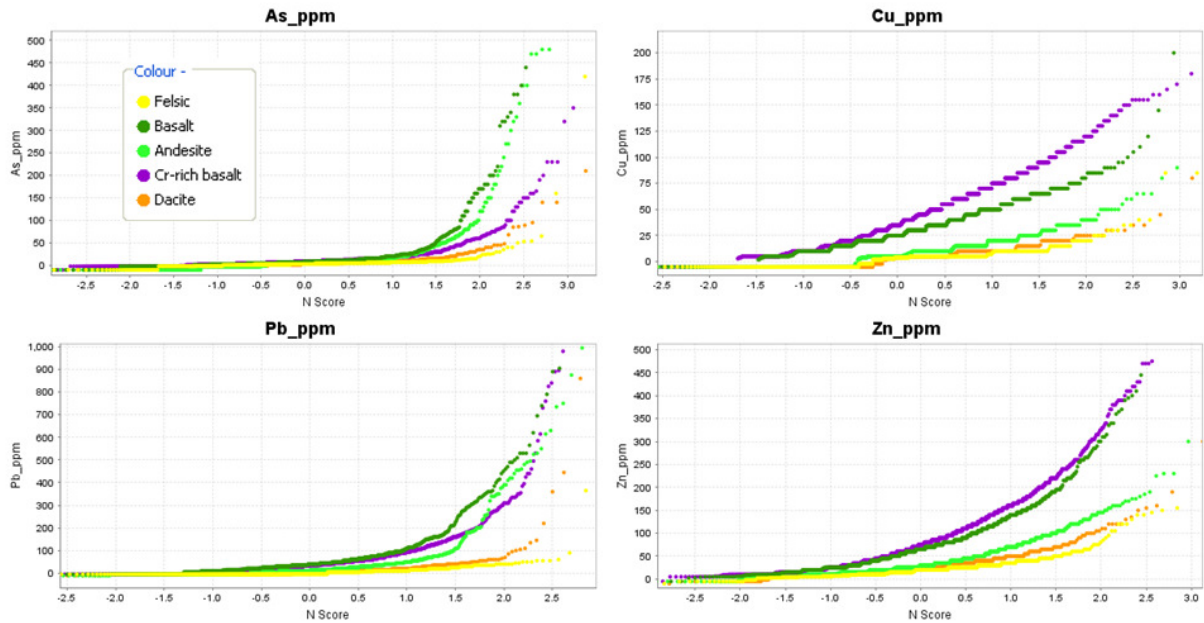


Figure 24.

The probability plots of As, Cu, Pb and Zn are particularly instructive. The background copper levels consistently increase as the host rock becomes more mafic. This is because of the correlation between Cu and Fe in silicate minerals. Anomalous points should plot as a sharp upward inflection in the probability plot. Very few copper results in this data set are anomalous. In contrast, arsenic shows some classic anomaly profiles. Zinc is similar to copper, but somewhat more anomalous in places. Lead also has some significant anomalies. The soil geochem is really showing the same picture that the lithochem provided. The arsenic anomalies are much more coherent and consistent than the Cu-Pb-Zn anomalies. The VMS systems are much better defined in this region by As than Cu-Pb-Zn. This is well demonstrated in figures 25 and 26. Arsenic defines the known VMS systems very effectively in the soil geochemistry, whereas copper is just mapping lithology. There are some zones, specifically in the Switchback area, High Point and South Mount Charter, which have coherent Pb-Zn anomalism, but lack the arsenic signature. This is a distinctly different metallogenic signature. It is worth investigating why these are different. Aberfoyle collect a large Pb isotope data base. It is worth looking to see if the Pb-Zn anomaly zones that are lacking in As have a different Pb isotope signature to the VMS mineralization.

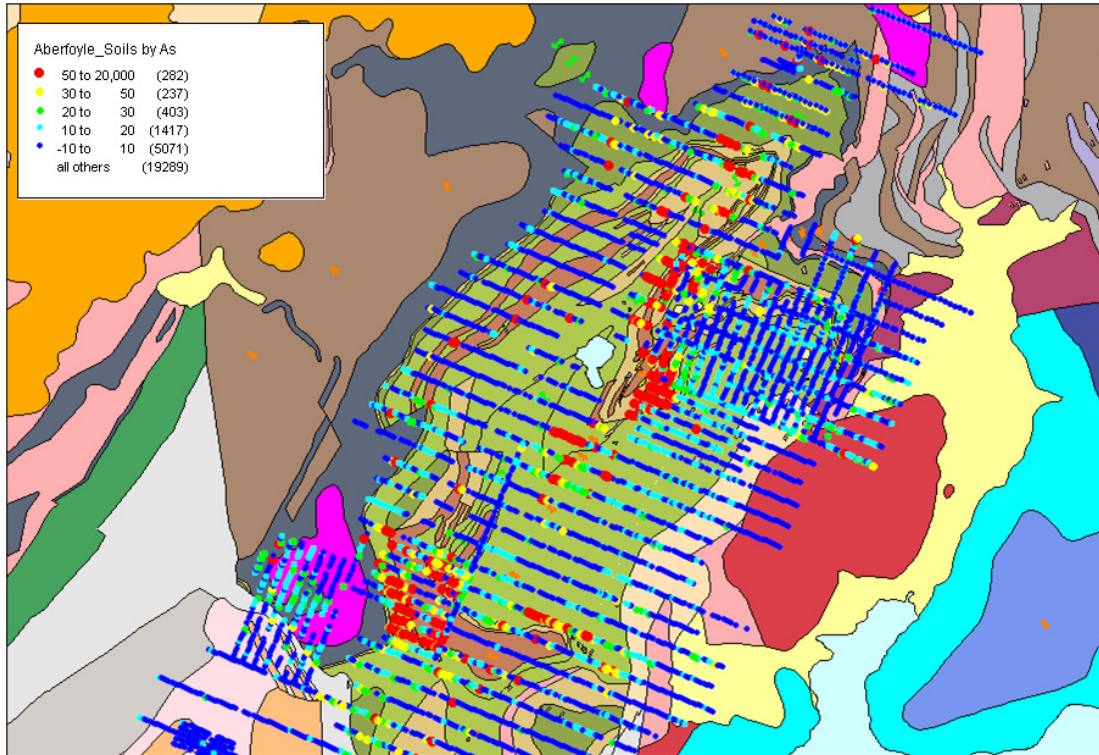


Figure 25. Map of Arsenic in soils.

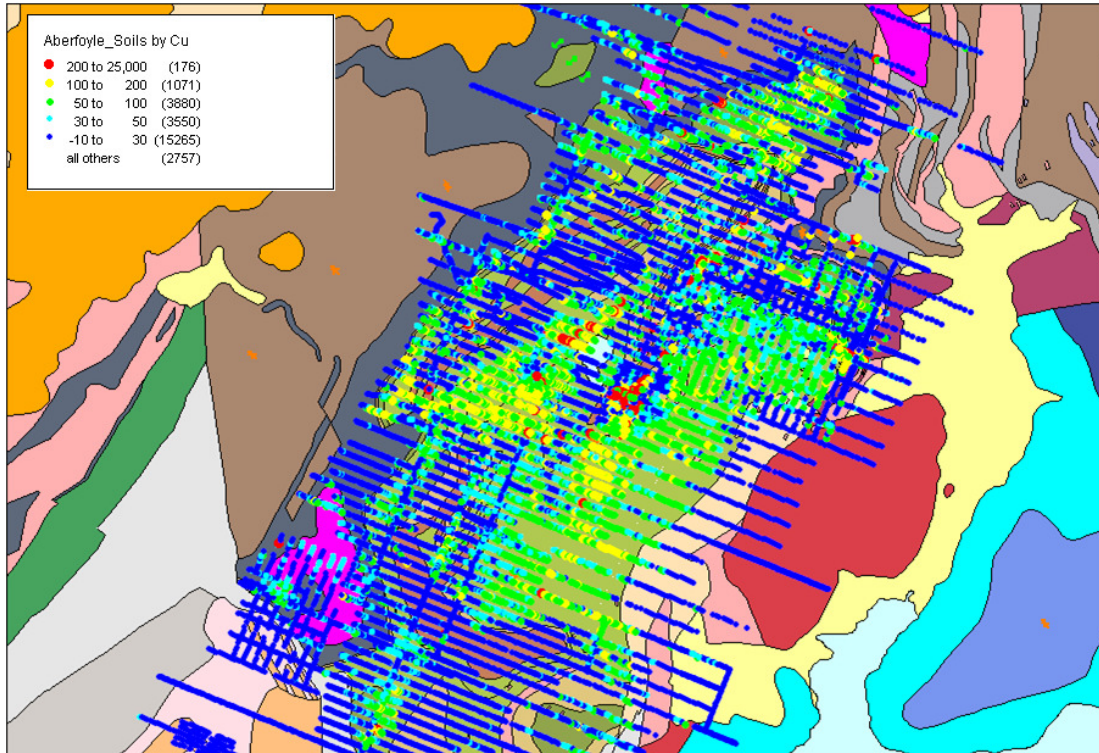


Figure 26. Map of Copper in soils.

## Signatures of Hellyer and Que River

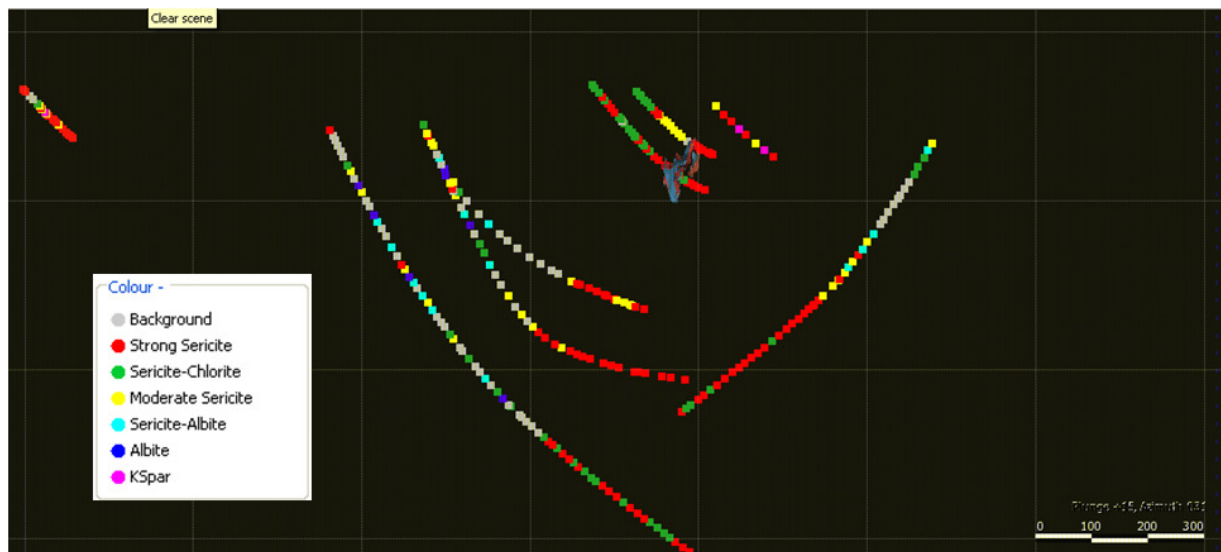


Figure 27. Que River Alteration Mineralogy

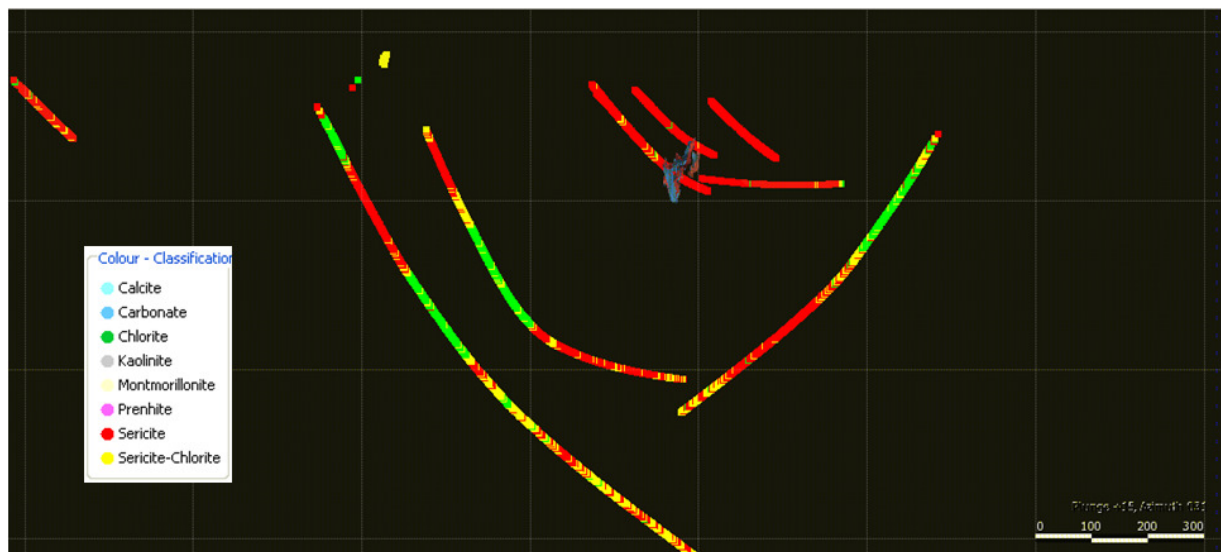


Figure 28. Que River ASD Mineralogy

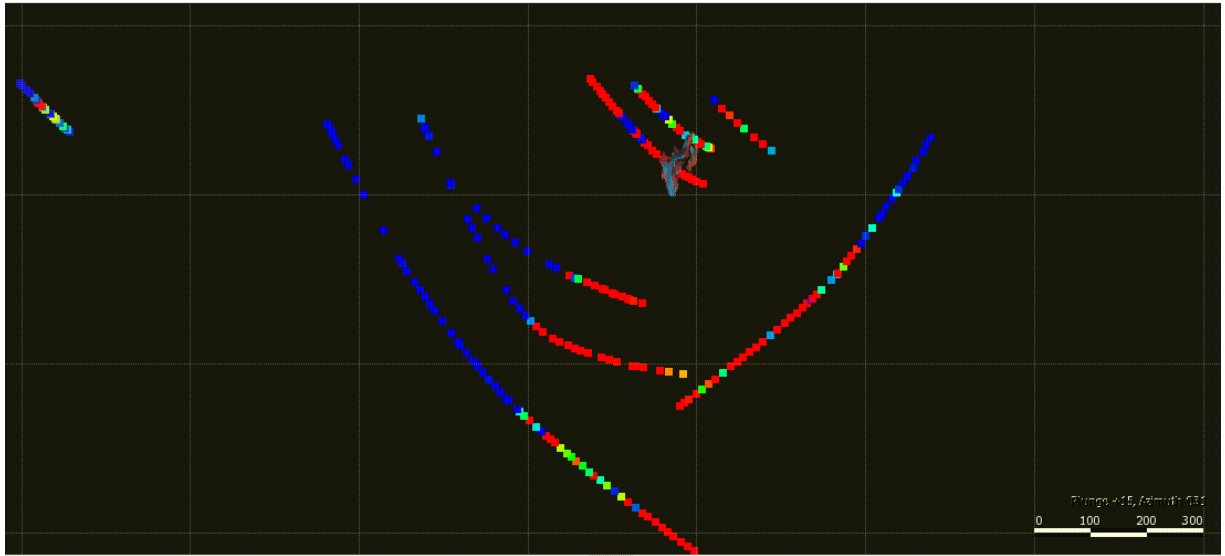


Figure 29. Que River Sulfur geochemistry.

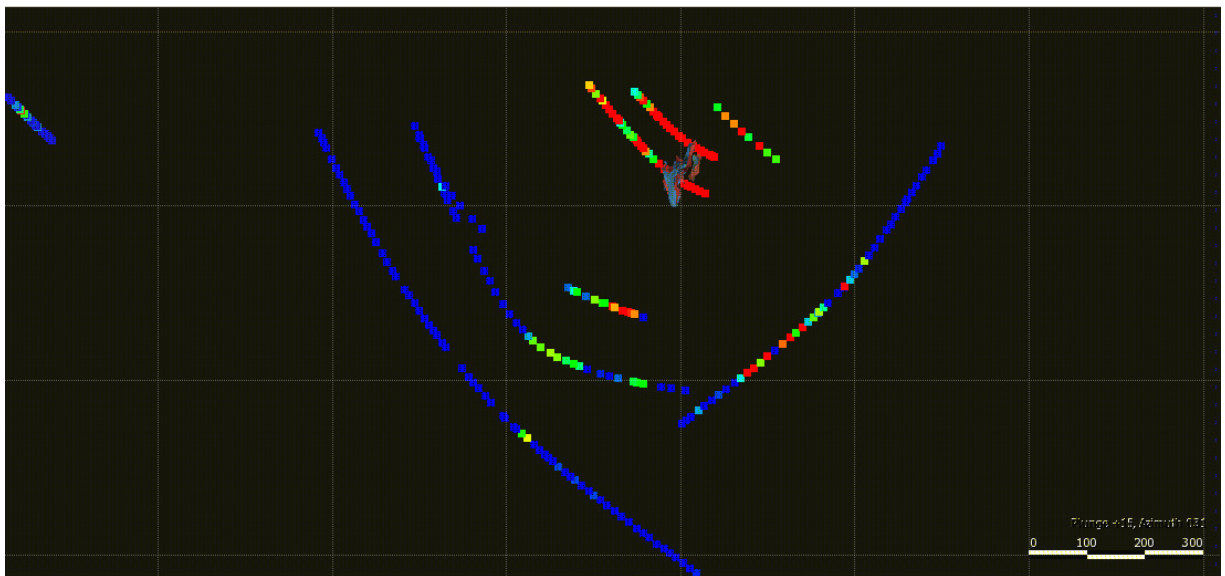


Figure 30. Que River Thallium geochemistry.

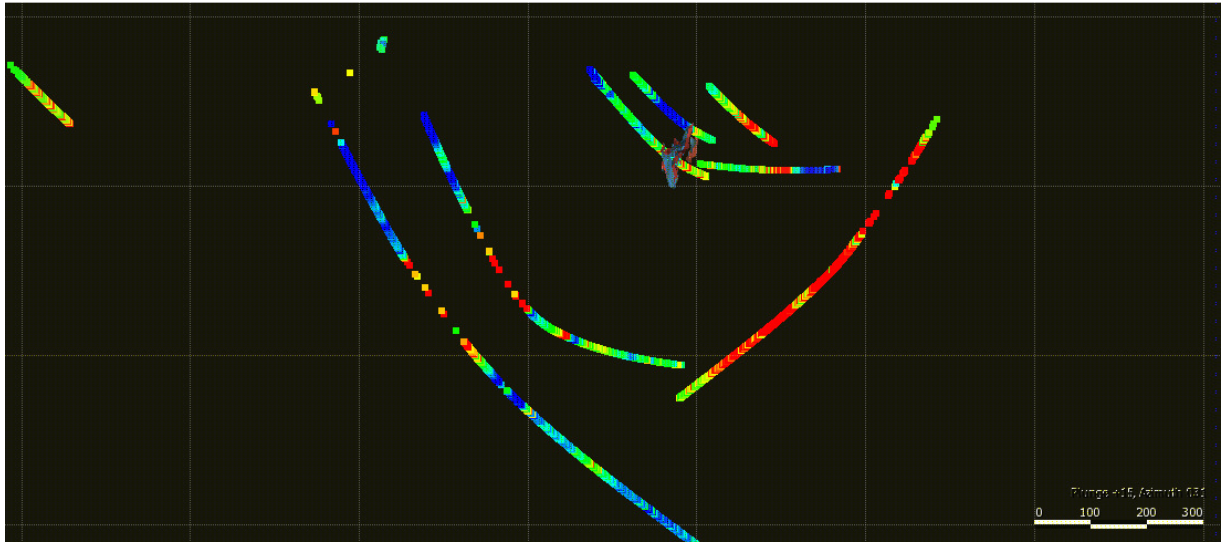


Figure 31. Que River sericite wavelengths. Blue<2200nm, Red>2215nm

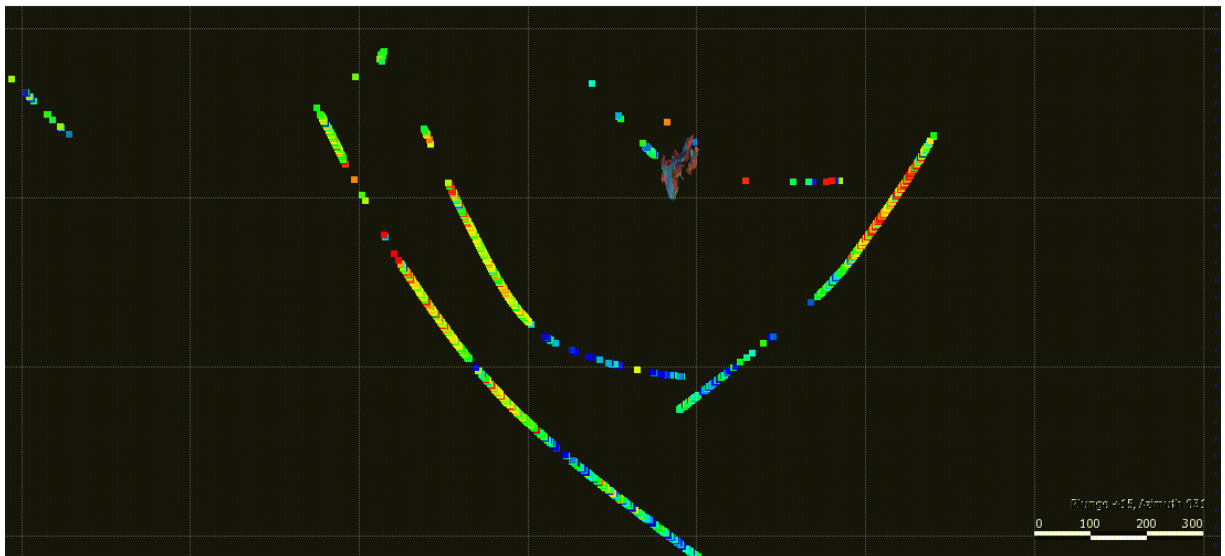


Figure 32. Que River chlorite wavelengths. Blue<2251nm, Red>2257nm



Figure 33. Hellyer Alteration Mineralogy

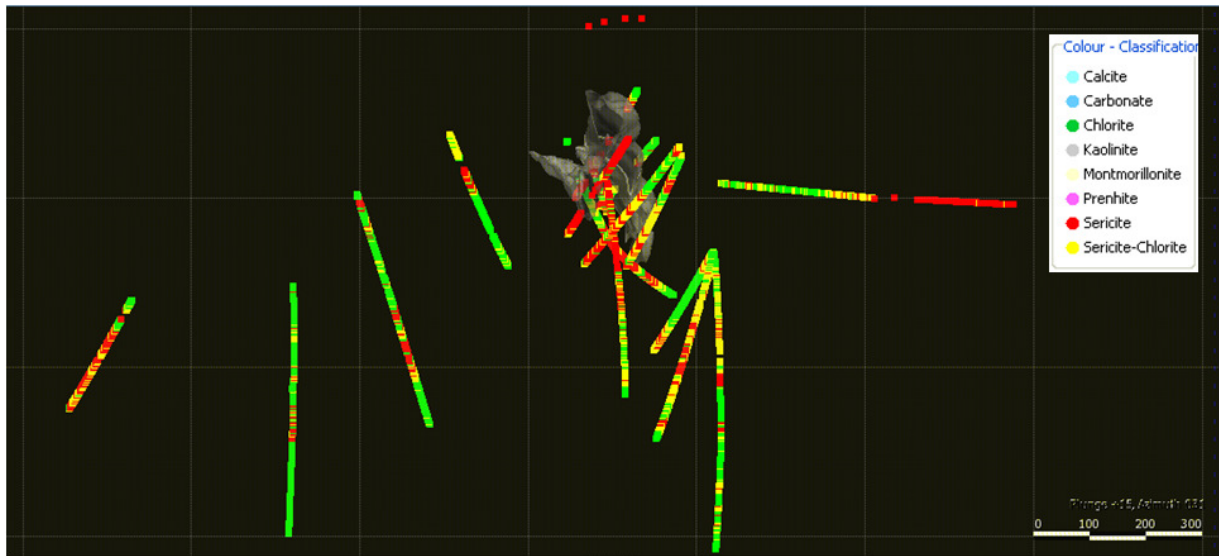


Figure 34. Hellyer ASD Mineralogy

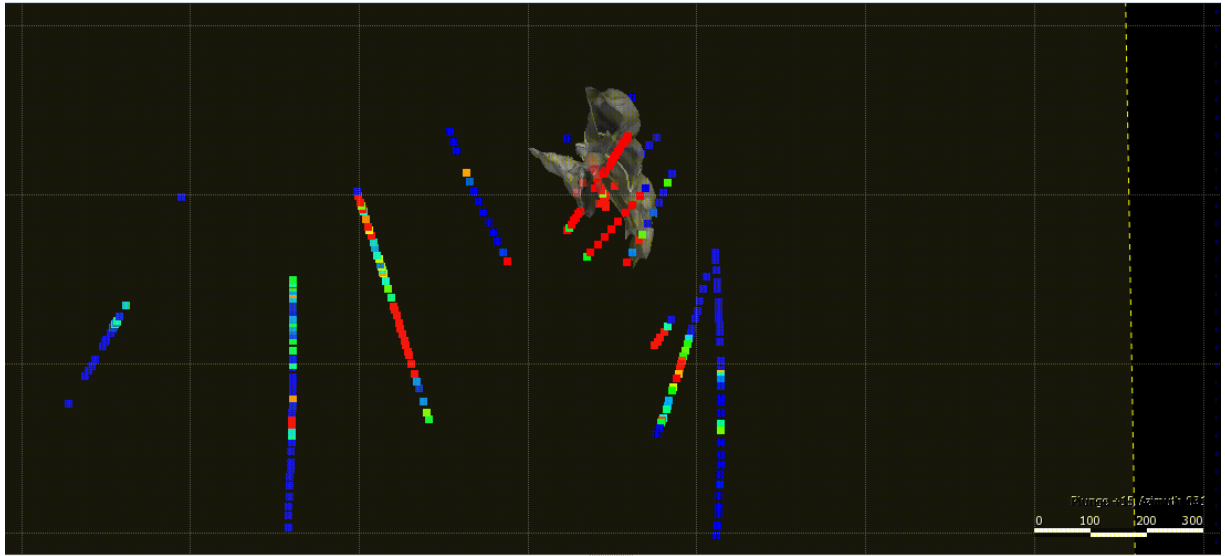


Figure 35. Hellyer Sulfur geochemistry.

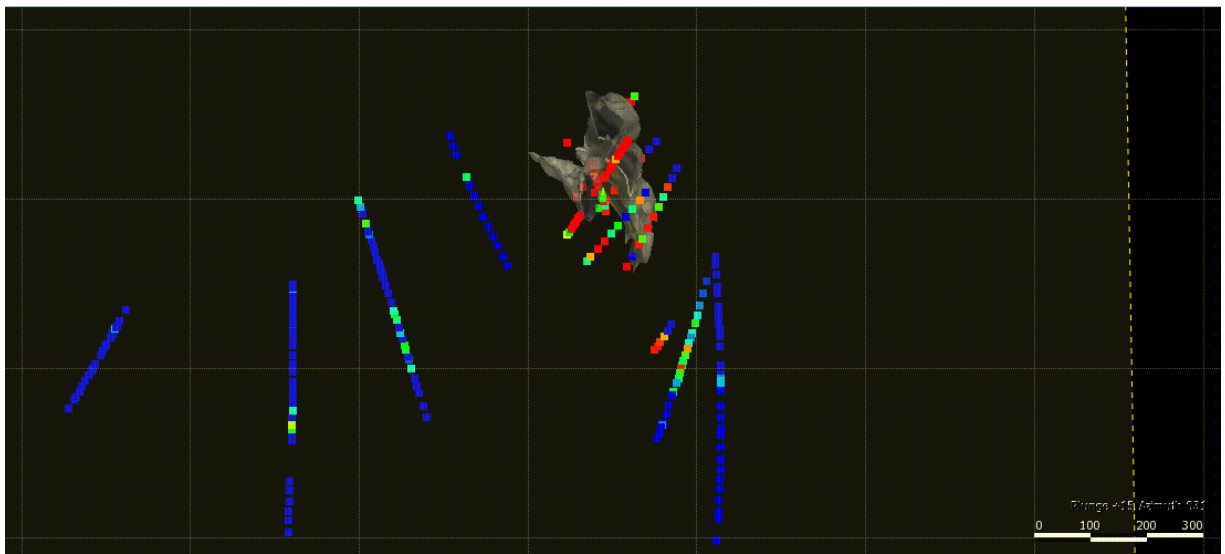


Figure 36. Hellyer Thallium geochemistry

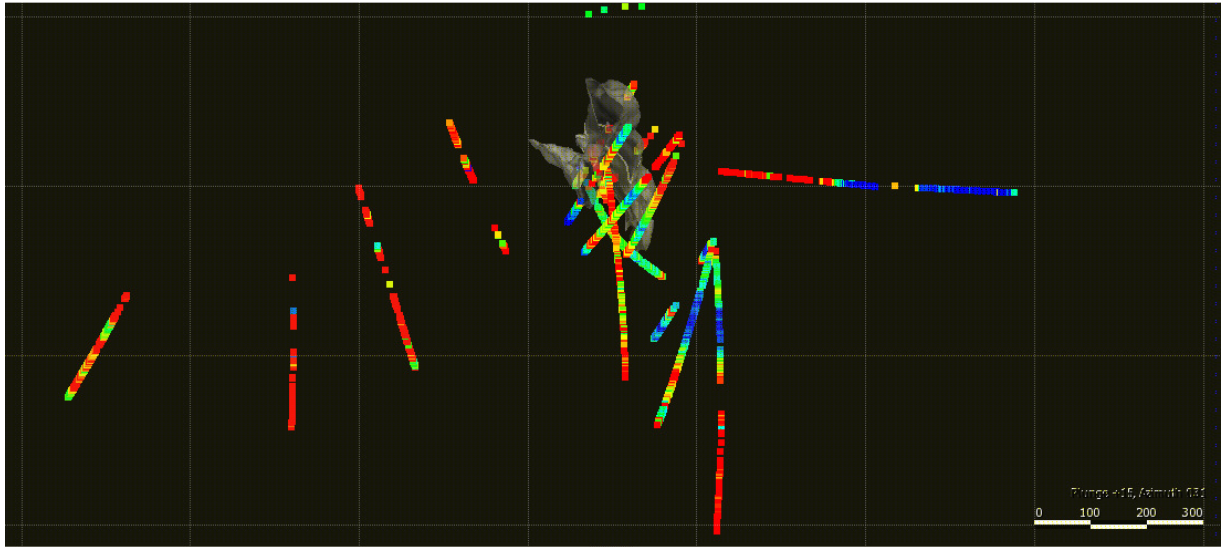


Figure 37. Hellyer sericite wavelengths. Blue<2200nm, Red>2215nm

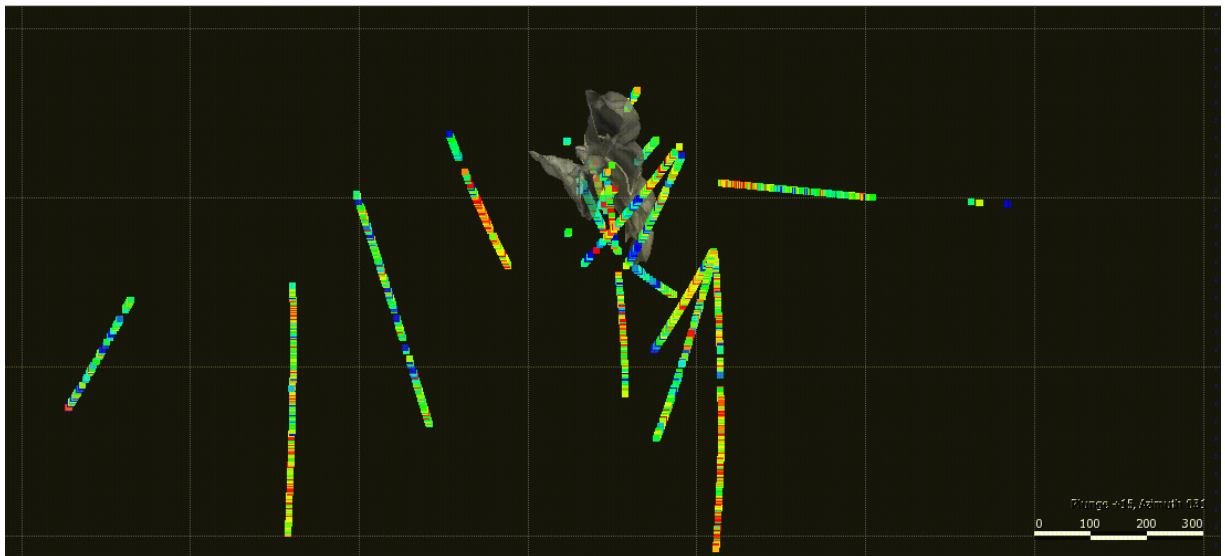


Figure 38. Hellyer chlorite wavelengths. Blue<2251nm, Red>2257nm

## Targets

### North of Hellyer

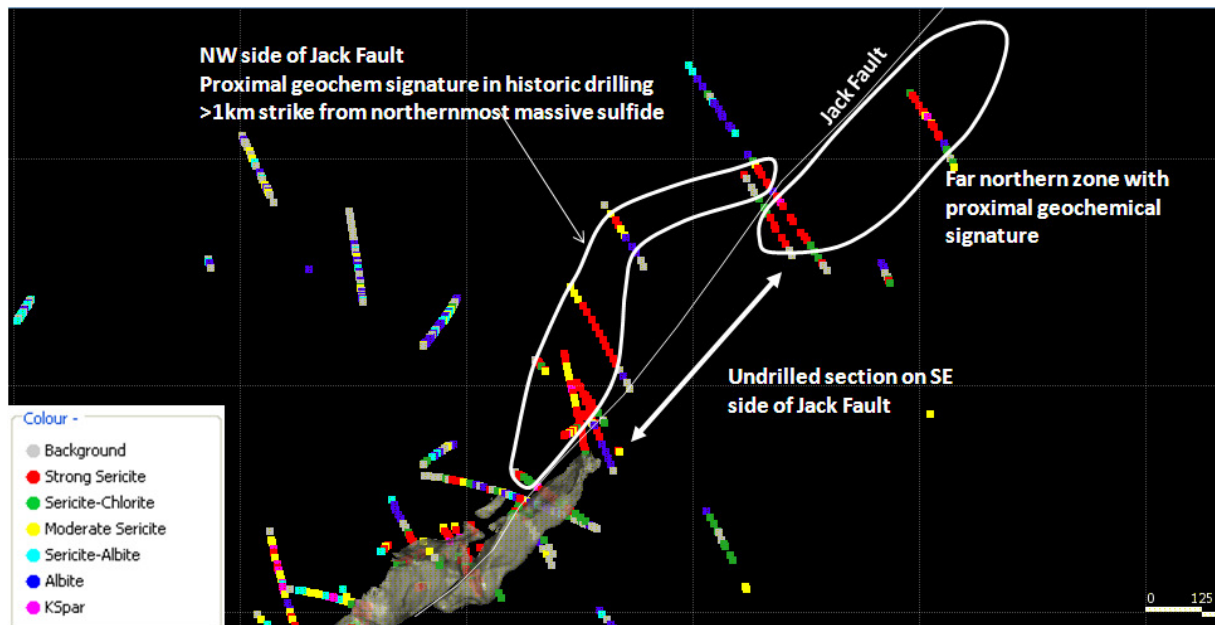


Figure 39. Target zones north of Hellyer; plan view.

The massive sulfide at the northern end of Hellyer is closed off by one line of drilling on either side of the Jack Fault. On the NW side of the Jack Fault, there are 6 drill holes in the next 1 km. All of these holes intersected footwall alteration with a very proximal signature. There is great potential here for another sulfide pod. Given the drill spacing, potential exists for a pod larger than Fossey. This zone has the intense footwall sericite and sericite-chlorite style alteration, with As-Sb-Tl values similar to that elsewhere in Hellyer. The previous holes were drilled at a shallow angle from the SE side through the stringer zone. Relogging and interpretation of the holes is required to ascertain whether they have in fact drilled through the HVS on top of the stringer zone, and see whether this position is still untested. Where the HVS has been tested, the pierce points should be plotted, so that the remaining untested surface area on top of the stringer can be mapped out. The down-side of this target is that the previous holes look very proximal, but the downhole EM did not detect a conductor.

On the SE side of the Jack Fault, the northern end of the sulfide lode has a relatively steep south-easterly dip. From the northern-most sulfide, there is a gap in the drilling of around 750m before there is another pierce point through the target stratigraphic/structural zone. It is certainly worth drilling one or two more holes into this zone.

The 4 most northern holes still have a very proximal geochemical signature, located either side of the northern extension of the Jack Fault. This is undoubtedly the same signature as the Hellyer system. However, the target here is starting to get very deep.

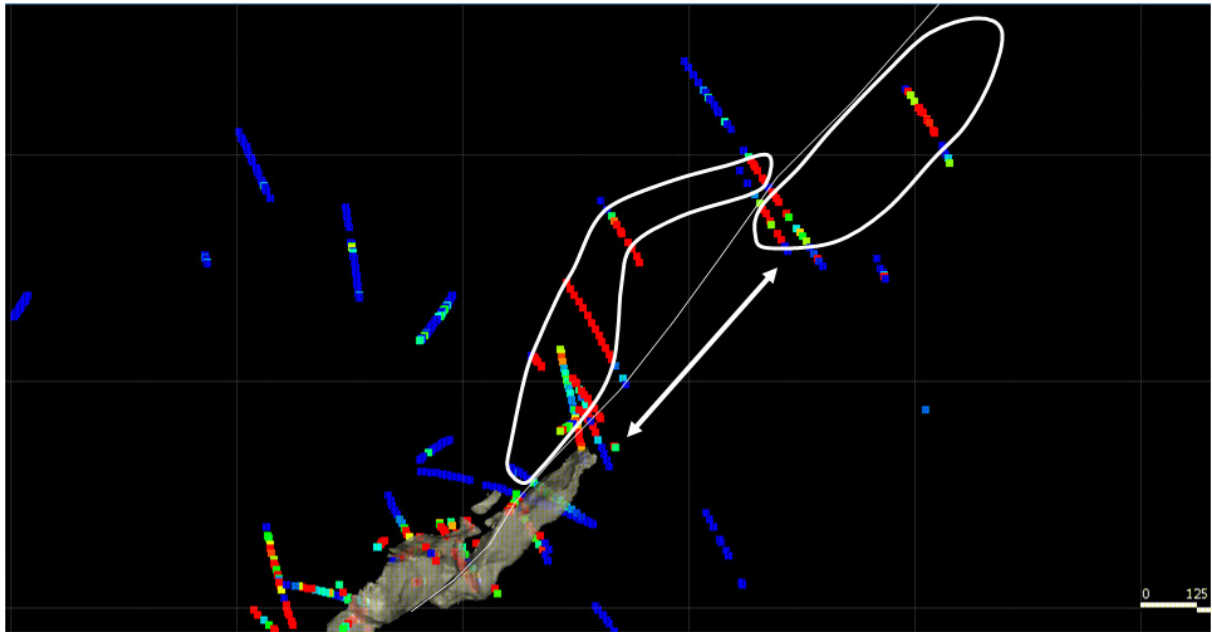


Figure 40. Target zones north of Hellyer; Thallium geochemistry; plan view.

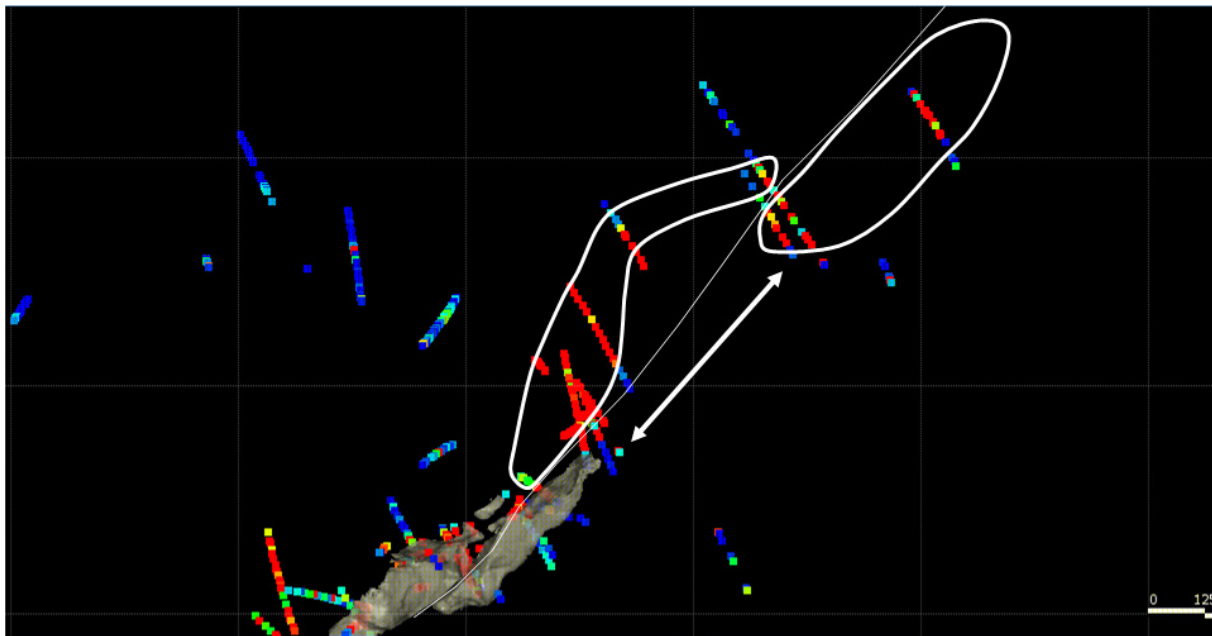


Figure 41. Target zones north of Hellyer; Arsenic geochemistry; plan view.

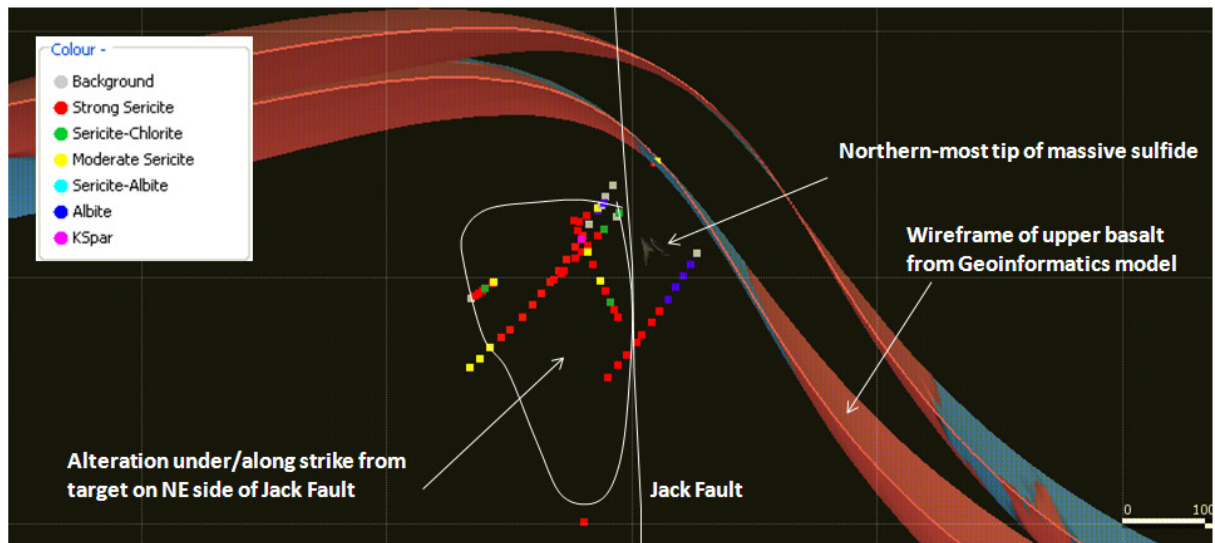


Figure 42. Alteration mineralogy north of Hellyer; section view.

### D Zone

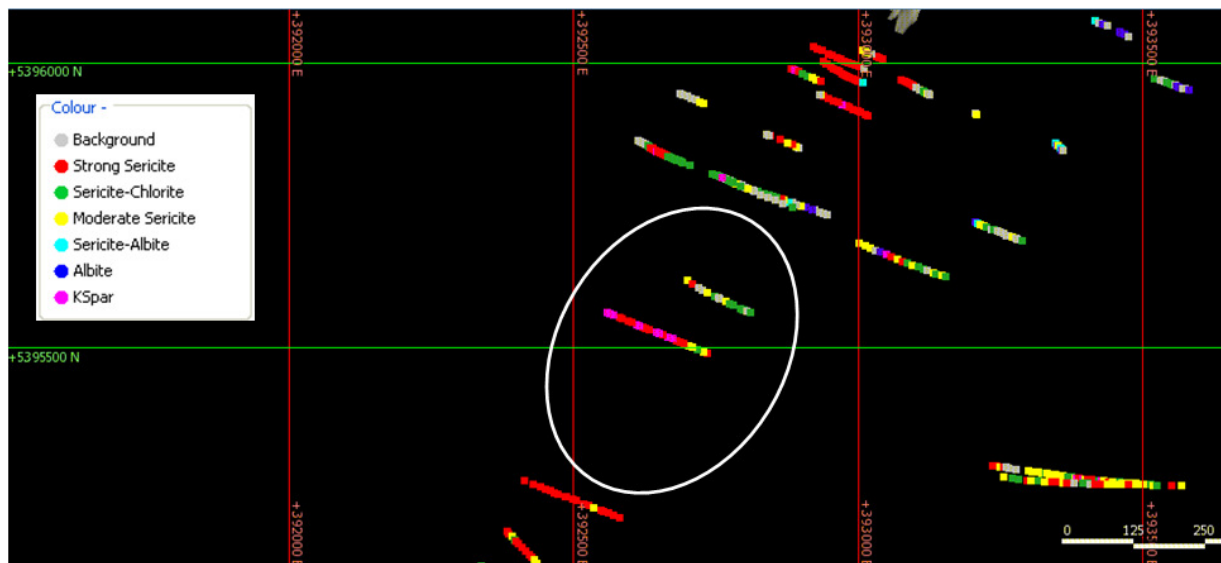


Figure 43. D Zone alteration mineralogy projected to plan view.

The “D-Zone” south of Fossey has a very strong proximal geochemical response. It has intense sericite, and the K feldspar signature, like Fossey, with strong As-Sb-Tl. The danger with this target is that the massive sulfide horizon has already been eroded off.

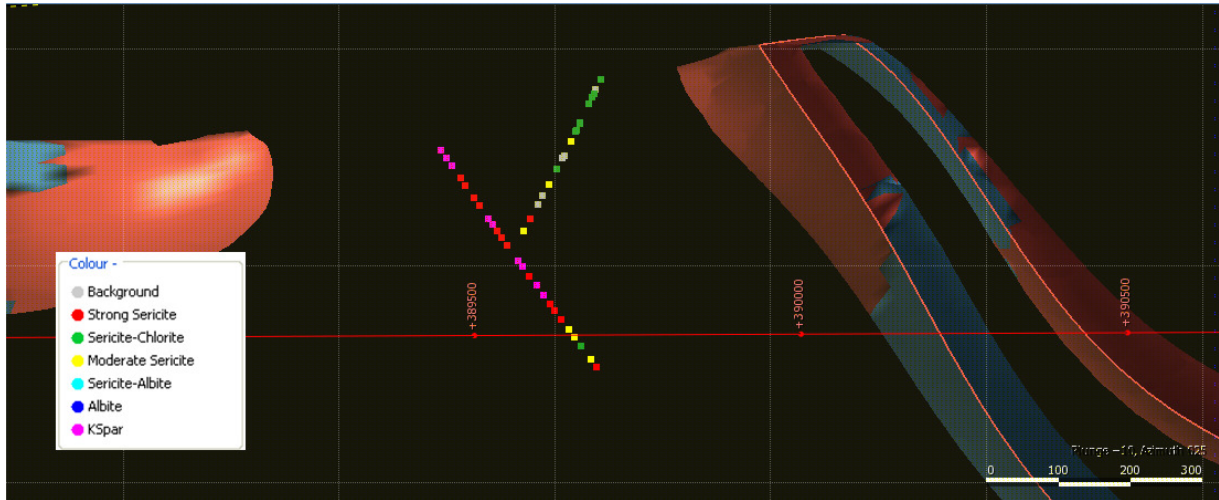


Figure 44. D Zone alteration mineralogy projected to section view. The shapes are the upper basalt from the Geoinformatics model.

### Que South

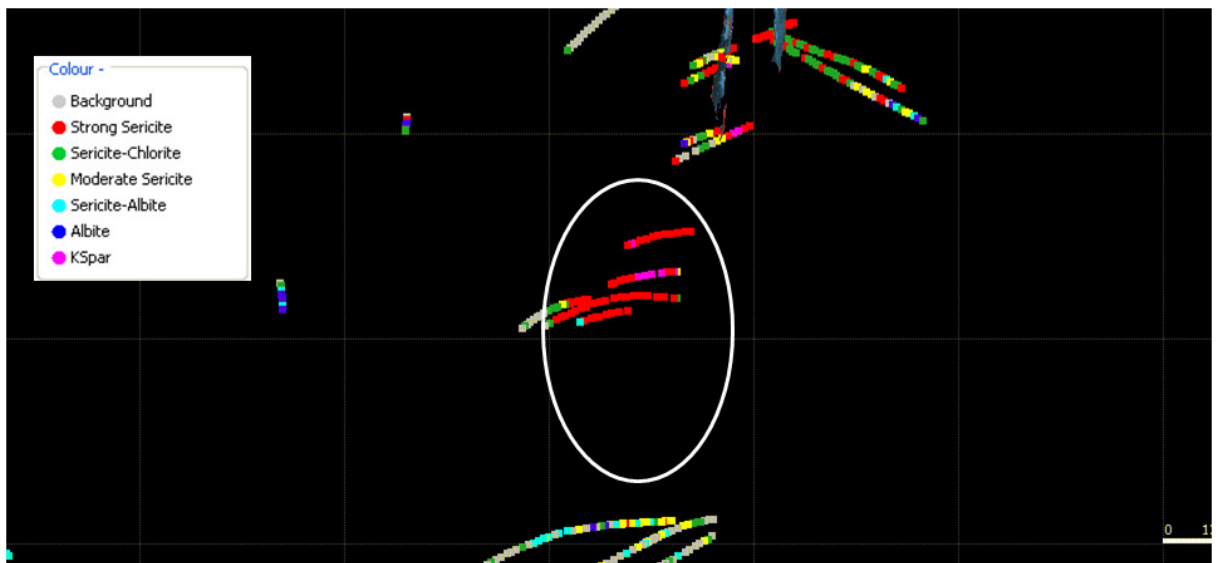


Figure 45. Alteration Mineralogy projected to plan view; Que South.

The southern end of the Que River alteration system south of the Mount Cripps Fault has a very proximal geochemical signature, with intense sericite alteration, K feldspar and strong As-Sb-Tl. It has been reasonably well drilled over a 200 to 300 meter strike length, but it still has some room to move. Again, some relogging and reinterpretation to create small scale 3D model is required, particularly to see whether the potential massive sulfide position has been eroded off.

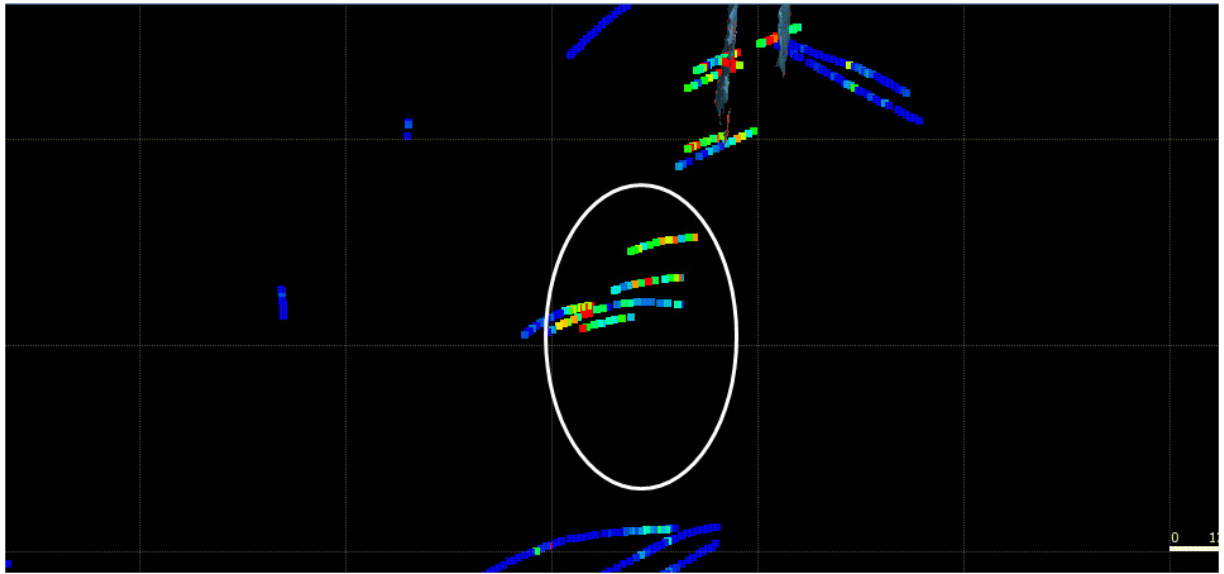


Figure 46. Antimony geochemistry projected to plan view; Que South.

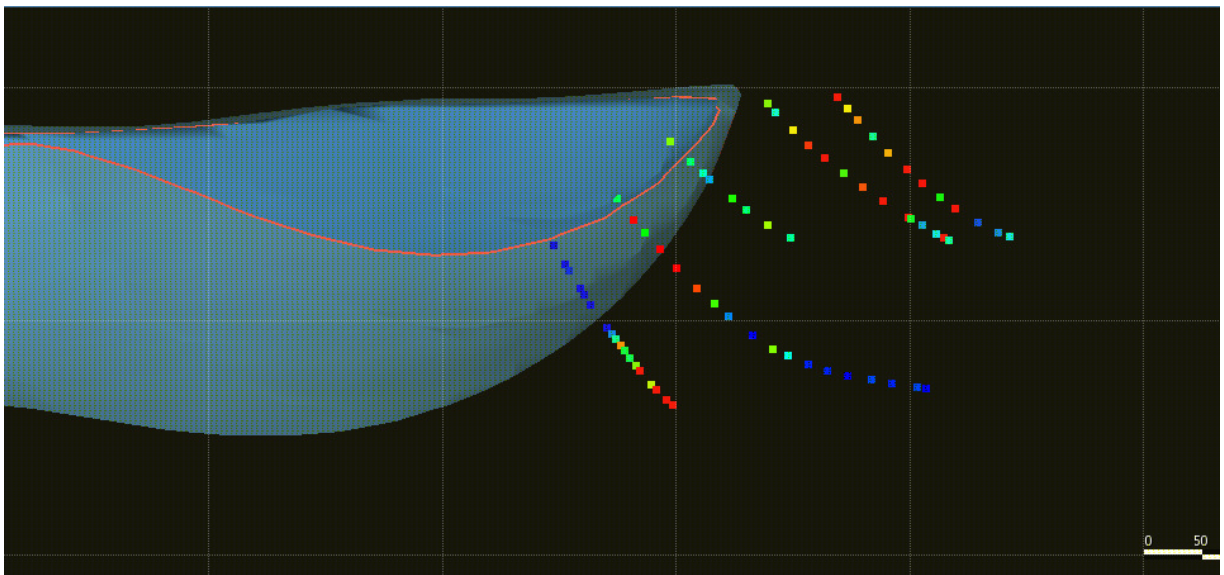


Figure 47. Que South Thallium geochemistry projected to a section. the shape is the upper basalt from the Geoinformatics 3D model.

## HL629

The strongest “near-miss” signature outside the main Hellyer to Mt Charter corridor is in drill hole HL629. Perhaps the most significant factor about the alteration in this hole is the 200 meter width of strong to moderate alteration. This is more substantial than any of the other target zones outside the main corridor. Also, there is remarkably little drilling within the vicinity of this hole.

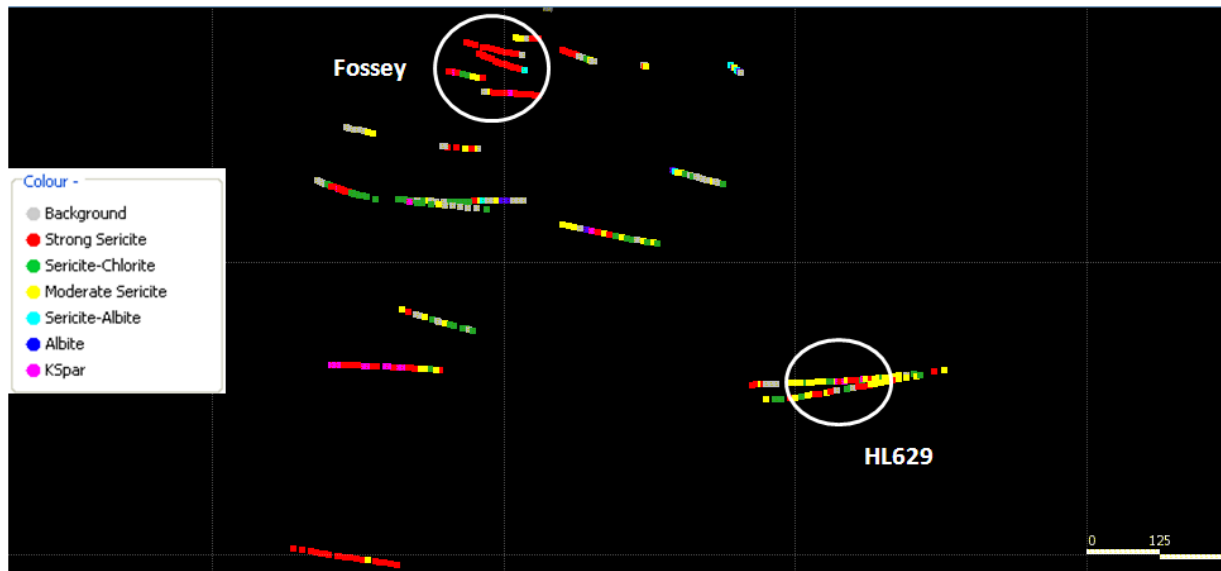


Figure 48. HL629 alteration geochemistry projected to plan view.

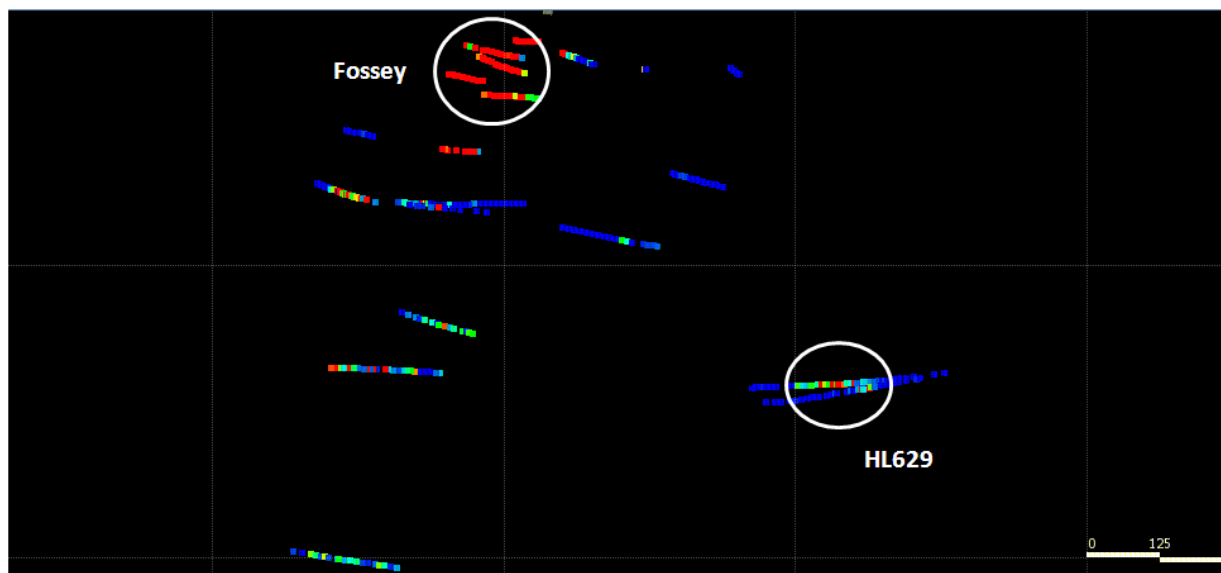


Figure 49. HL629 Thallium geochemistry projected to plan view.

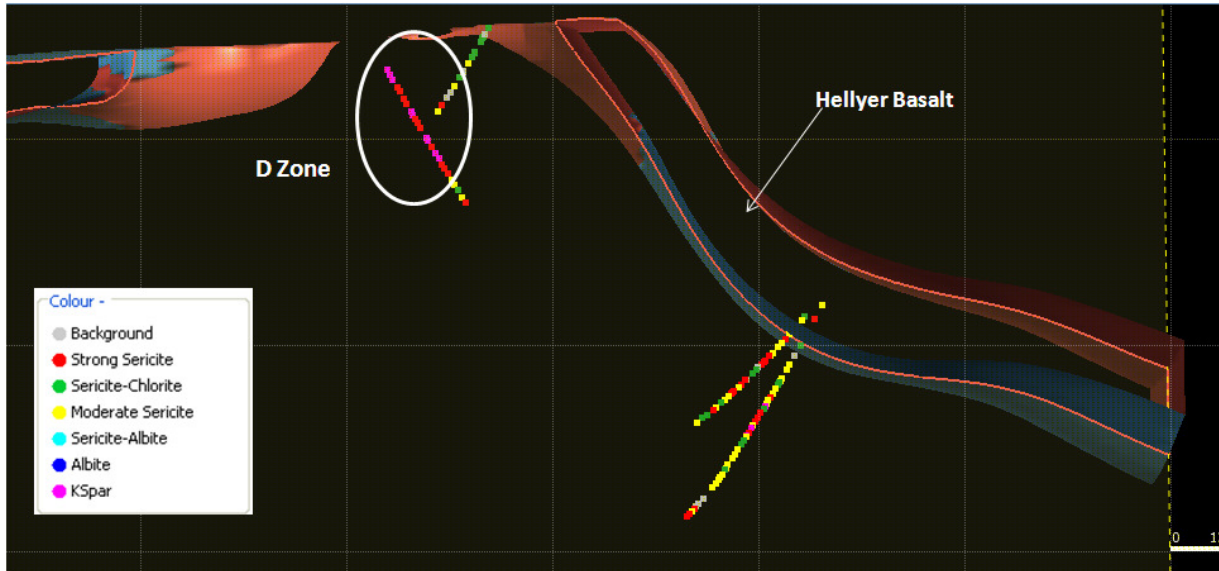


Figure 50. HL629 alteration mineralogy projected to cross section. The shape is the upper basalt from the Geoinformatics 3D model.

### Switchback Zone

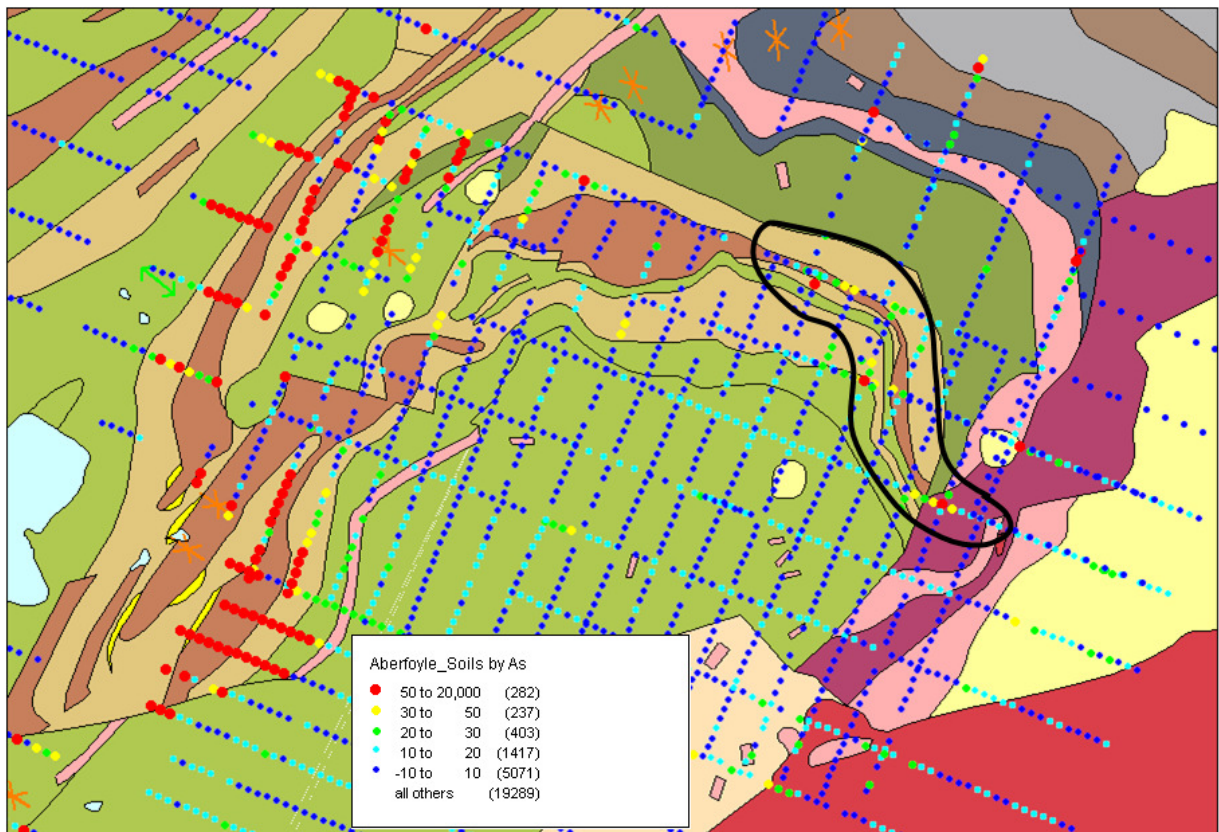


Figure 51. Arsenic soil geochemistry across the Switchback Zone.

The Switchback zone is located along the mixed volcanoclastic sequence NE of Que River, where it runs into the Henty Fault/Mt Cripps fault confluence. The whole area is pervasively moderately sericite-chlorite altered, even into the hangingwall rocks. The soil geochemistry shows a narrow, but continuously mineralized position running along the surface trace of the mixed volcanoclastic sequence. Drillhole HED12 intersected an intensely altered and quite well mineralized interval in the mixed volcanoclastic sequence. However, the width and nature of the alteration is consistent with the arsenic pattern displayed in the soil geochemistry at surface. This still looks like a reasonable target area, but it would be good to see a larger volume of strongly altered rock.

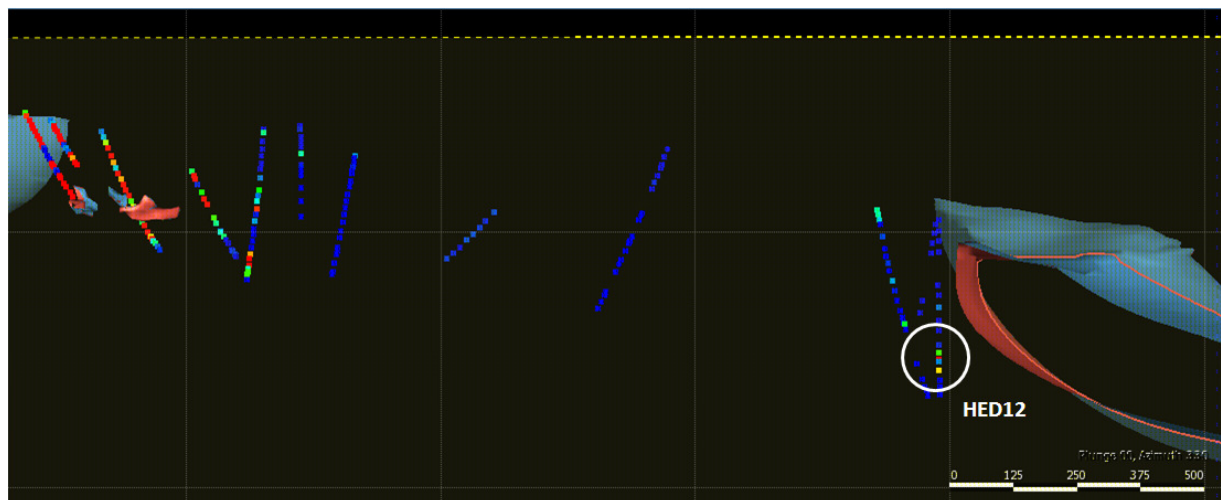


Figure 52. Arsenic geochemistry in HED12, Switchback area.

### Amoeba Zone

The mixed volcanoclastic sequence is exposed in the hinge of the westernmost anticline of Que-Hellyer volcanics. This is a mapped alteration zone at surface. It also has an expression in the soil geochemistry, being a narrow and apparently continuous arsenic anomaly. The nature, thickness and tenor of the alteration intersected in the few DDH's in this zone are consistent with the pattern displayed in the arsenic soil geochemistry. There is however, a large subsurface area of this host unit between the Amoeba Zone and Que River. The best options for testing this are to drill stratigraphic holes to get more vectoring information, or employ a more sensitive airborne EM method.

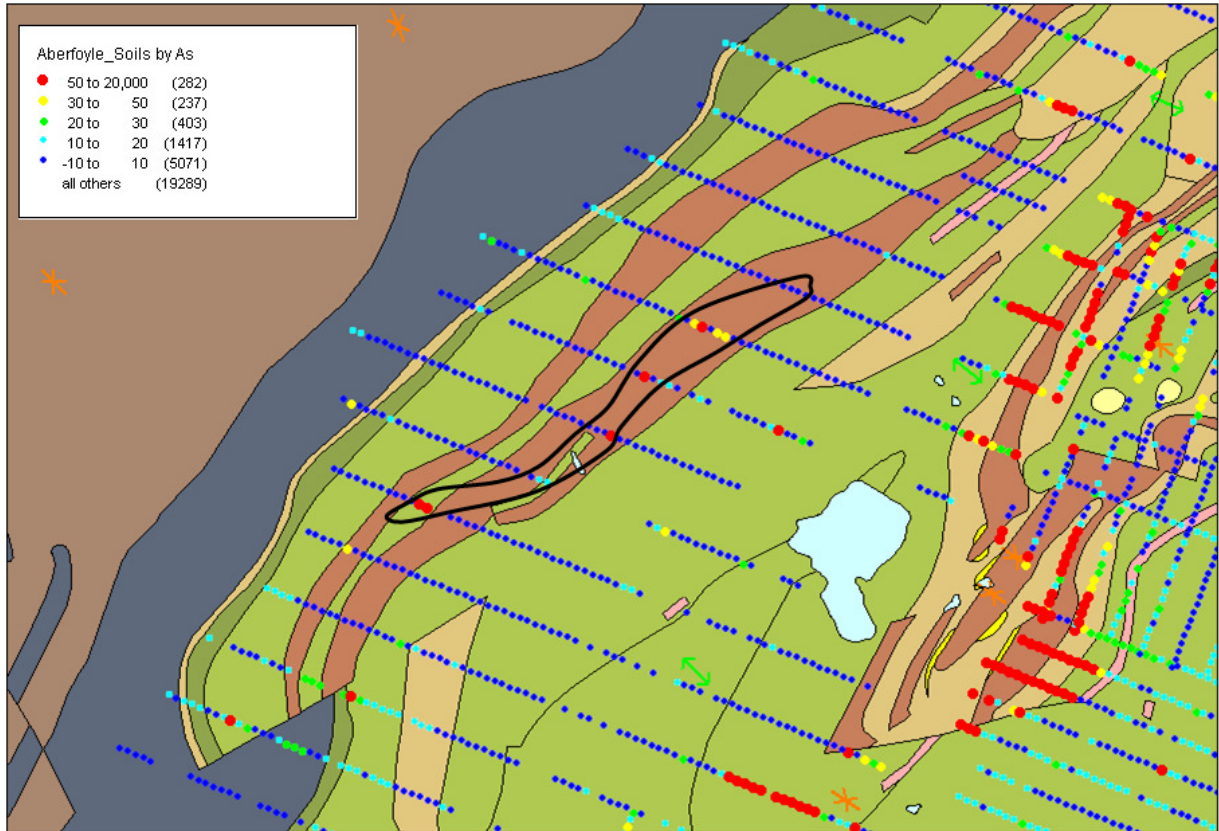


Figure 53. Arsenic soil geochemistry; Amoeba Zone.

**Barite Creek**

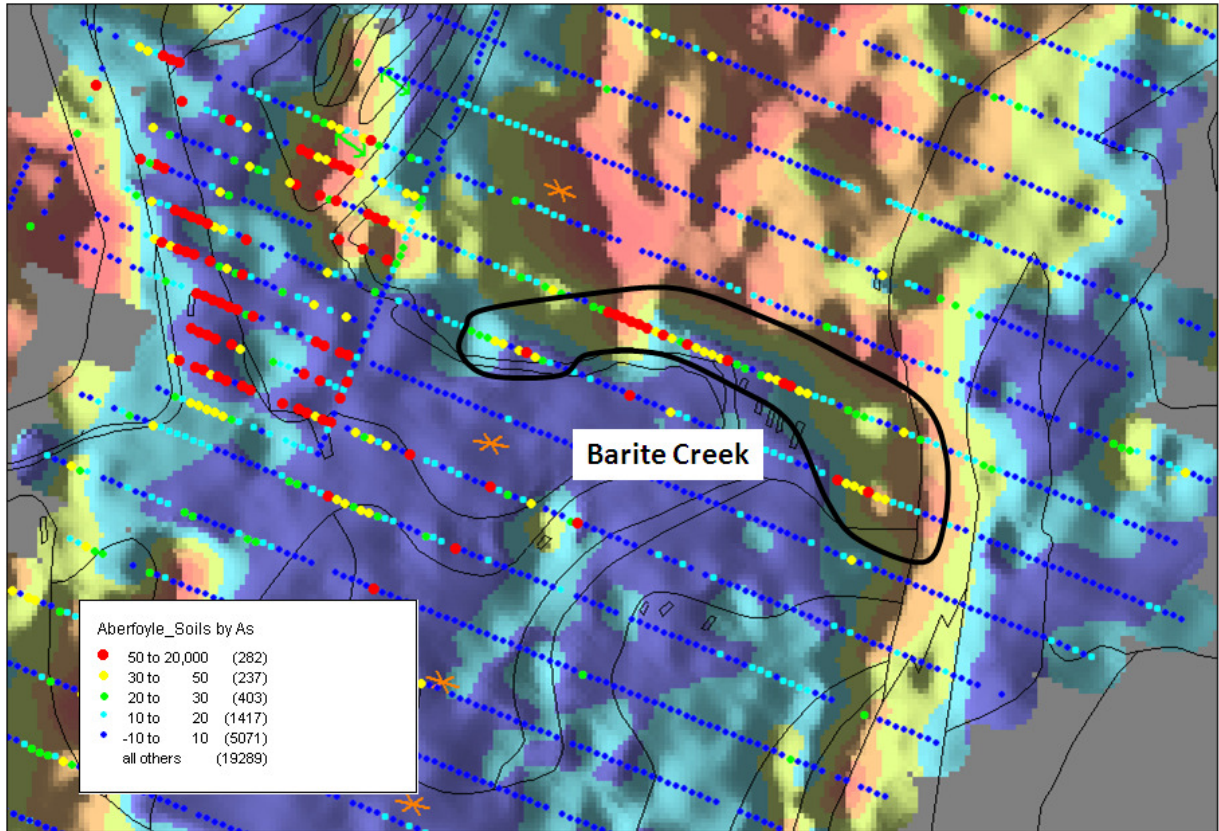


Figure 54. Arsenic soil geochemistry; Barite Creek.

## References

Crawford, A.J., Corbett, K.D. and Everard, J.L., 1992. Geochemistry of the Cambrian Volcanic-Hosted Massive Sulfide-Rich Mount Read Volcanics, Tasmania, and Some Tectonic Implications. *Economic Geology*, VOLUME 87 / NUMBER 3, 597-619